Growth of Gel Microstructures between Stressed Silica Grains and its Effect on Soil Stiffening

by

Rui Guo

Department of Civil and Environmental Engineering
Duke University

Date:_____

Approved:

_____
Tomasz A Hueckel, Supervisor

_____
Piotr E Marszalek

_____
Fred K Boadu

_____
Joseph C Nadeau

_____
Xuanhe Zhao

Thesis submitted in partial fulfillment of
the requirements for the degree
Master of Science in the Department of
Civil and Environmental Engineering in the Graduate School
of Duke University

2013

ABSTRACT

Growth of Gel Microstructures between Stressed Silica Grains and its Effect on Soil Stiffening

by

Rui Guo

Department of Civil and Environmental Engineering
Duke University

Date:_____

Approved:

_____
Tomasz A Hueckel, Supervisor

_____
Piotr E Marszalek

_____
Fred K Boadu

_____
Joseph C Nadeau

_____
Xuanhe Zhao

An abstract of a thesis submitted in partial
fulfillment of the requirements for the degree
of Master of Science in the Department of
Civil and Environmental Engineering in the Graduate School of
Duke University

2013

Abstract

Laboratory tests on microscale are reported in which two amorphous silica cubes were compressed in a liquid environment, namely in solutions with different silica ion concentrations for up to four weeks. Such an arrangement represents an idealized representation of two sand grains. The grain surfaces and asperities were examined in Scanning Electron Microscope (SEM) and Atomic Force Microscope (AFM) for fractures, silica gel growth, and polymer strength. In 500ppm solution, silica gel structures a few hundred microns long appeared between stressed silica cubes. In 200ppm solution, silica deposits were found around damaged grain surfaces, while at 90ppm (below silica solubility in neutral pH), fibers a few microns in length were found growing in cube cracks. AFM pulling tests found polymers with strength in the order of 100nN and length between 50 and 100 nm. After aging, size of silica gel is in the order of 10-100 μm with intergranular strength in the order of 0.01-1 mN. We concluded that prolonged compression produced damage in grains, raising local Si ion concentration, and accelerating precipitation, polymerization and gelation of silica on grain surfaces enhancing soil strength at the microscale, hence most likely contributing to the aging phenomenon observed at the macroscale. Mica surfaces near stressed silica contacts were also found to enhance silica gel growth.

Dedication

To my parents, who made me who I am, and my wife, who is always there for me.

Contents

Abstract iv

List of Figures vii

Acknowledgements x

1. Introduction 1

2. Objectives and tasks 9

3. Literature review 12

4. Experimental methods 19

   4.1. Silica gel studies 21

   4.2. Pneumatic grain crushing 23

   4.3. Spring cube crushing 27

   4.4. Micro-strain testing 31

   4.5. Consolidation testing 32

5. Preliminary results 34

   5.1. Growth of silica gel in solution 34

   5.2. Growth of silica gel near stressed contacts 37

   5.3. Tensile strength of silica polymers 43

   5.4. Strength of silica gel between grains 45

   5.5. Mica-induced silica gel growth 54

6. Discussion and conclusions 63

7. Future work 70

Bibliography 72

List of Figures

Figure 1: Granular assembly of sand grains....20

Figure 2: Configuration of silica cubes in cube crushing experiments....24

Figure 3: A CAD rendering of the pneumatic cube crushing apparatus....25

Figure 4: Detailed configuration of the fluid chamber in pneumatic cube crushing apparatus....26

Figure 5: Schematics of spring cube crushing apparatus....28

Figure 6: Spring cube crushing apparatus attached to load frame and analytic scale....30

Figure 7: AFM image of 300 ppm Si ion concentration solution after 7 days....34

Figure 8: AFM image of 300 ppm Si ion concentration solution after 15 days....34

Figure 9: AFM image of 180 ppm Si ion concentration solution after 7 days....35

Figure 10: AFM image of 150 ppm Si ion concentration solution after 2 weeks....36

Figure 11: Silica aerogel, gold coated, magnification x97....37

Figure 12: Internal structures of silica aerogel. Magnification x5174....37

Figure 13: Silica polymers near contact between two silica cubes in 500 ppm Si ion concentration pH 5.0 solution after 3 weeks....38

Figure 14: Energy Dispersive X-ray Spectrometer composition analysis of structures in Figure 13....39

Figure 15: Silica gel growth near silica cube aged for 4 weeks in 500 ppm Si ion concentration pH 5.0 solution....40

Figure 16: Silica deposits in silica cube crack after 2 weeks aging in 300 ppm Si ion concentration pH 5.0 solution....41

Figure 17: Clean cube surfaces after 2 weeks aging in 300 ppm Si ion concentration pH 5.0 solution....41

Figure 18: Silica gel growing on cube surfaces after 3 weeks aging in 200 ppm Si ion concentration pH 2.5 solution 42

Figure 19: Thin polymers connecting silica gel to cube surface, seen in 200 ppm Si ion concentration pH 2.5 solution after 3 weeks aging 42

Figure 20: Silica polymer growth in 90 ppm Si ion concentration pH 5.0 solution after 3 weeks aging 43

Figure 21: AFM force curves on cube surface in 210 ppm Si ion concentration pH 5.0 solution for 2 weeks 44

Figure 22: AFM force curve on silica cube surface with no polymers picked up 45

Figure 23: Adhesive force against cube displacement for cubes in 500 Si ppm pH 5.0 solution for 3 weeks 46

Figure 24: Force-Displacement curve around the peak 47

Figure 25: Force-Displacement curve for control experiment 48

Figure 26: Another Force-Displacement curve in 500 ppm solution 49

Figure 27: Difference in force magnitude between consecutive measurements 50

Figure 28: Force-displacement curve, 300 Si ppm, pH 2.7, 3 weeks 51

Figure 29: A closed up of a section of force-displacement curve 51

Figure 30: Difference in force magnitudes between measurements 52

Figure 31: Force-displacement curve of MSA test 1 53

Figure 32: SEM image of cube surface after MSA test 1 53

Figure 33: Force-displacement curve for MSA test 2 54

Figure 34: SEM image of cube-muscovite contact after aging 55

Figure 35: SEM image of mica sheet compressed between silica cubes 56

Figure 36: SEM image of cube surface after compression with mica sheet 57

Figure 37: SEM image of silica polymers on mica sheet near stressed contact 58

Figure 38: Force-displacement curve of cubes aged with mica sheet, Si 300 ppm 59

Figure 39: A section of force curve in Figure 38 59

Figure 40: Difference in force magnitude in aging with mica measurements..... 60

Figure 41: Force-displacement curve of cubes aged with mica, pH 5.0 61

Figure 42: SEM image of silica-mica contact after 3 weeks aging in pH 5.0 Si 300 ppm solution 61

Figure 43: Hydrated silica polymers near contact in SEM wet mode 62

Acknowledgements

I am heartily thankful to my advisor, Professor Tomasz Hueckel, whose encouragement, guidance and support made this work possible.

I also offer my regards to all of those who supported me in any respect during my research on the project.

Guo Rui

1. Introduction

Soil exhibits significant stiffening when subjected to a prolonged compression at a constant load in wet conditions. This effect is known under the name of soil aging and has been subject of interest for decades (Mitchell and Solymar 1984, Schmertmann 1991, Hueckel et al. 2001, Hueckel et al. 2005). While the phenomenon has been extensively measured in the field and in the laboratory experiments, the mechanisms behind soil aging and variables controlling it remains a subject of intense research (Baxter and Mitchell 2004). Aging in dry clean sand is attributed to creep or secondary consolidation of sand. It is suggested that particles continuously rearrange until stable equilibrium positions are reached under applied load and kinematic constraints (Mesri et al. 1990, Schmertmann 1991, Bowman and Soga 2003, Wang et al. 2008). The presence of fines in dry sand soils also increases creep strain and aging rate (Wang and Tsui 2009). Mechanical properties of granular assemblies at macroscopic level are known to be affected by contact networks, on one hand, and the local response of grain contact neighborhoods on the other (Parry 2004). In the latter case, the response is determined not only by the material itself, but also by how grains of the material interact with each other under stress. Such interactions are not purely mechanical, but are coupled with chemical processes such as dissolution, precipitation, polymerization and gelation of materials around contact region (Hu and Hueckel 2007a, Hu and Hueckel 2007b, Soulie

et al. 2007). Therefore, we claim that from strain and stress alone one cannot accurately predict the long-term mechanical properties of even perfectly granular materials.

Grain material in a stressed and submersed contact area undergoes two distinct stages of evolution of our interest; i.e. beyond the range of the grain elastic deformation. In the first stage, past the elastic limit, the grain in the zone of contact exhibits micro-cracking resulting in an inelastic deformation. In the second stage, mass dissolution rate increases as a result of an extra inter-phase interface surface area generated through micro-cracking. The softening of the grain due to mass dissolution is counterbalanced by irreversible straining. In nature, the processes of dissolution and redistribution of mass in granular media may occur on the geological timescale, such as the formation of sandstone by amorphous mass that binds the sand grains together (Worden and Morad 2000). However, experiments and various engineering geotechnologies have shown that such processes can also occur on a time scale of weeks or months (Denisov and Reltov 1961, Meyer et al. 2006, Hu and Hueckel 2007b).

Silica is the most abundant element in the Earth's crust. Common soil is made mostly of sand, which in turn is mostly quartz or SiO_2. Although quartz is almost insoluble in water (Iler 1955), experiments indicate that water presence and flow can significantly reduce the strength of quartz, though the mechanisms behind such phenomenon are still unknown (Gratier et al. 2009). However, it was also shown that in some cases the dissolution and re-deposition of silica at intergranular contact in sand

can improve the strength of quartz by as much as hundreds of kPa (Mitchell 1993). This water-silica paradox is partly what motivated this research.

One of the early hypotheses explaining the changes in strength of sand was put forward by Denisov and Reltov (1961), who conducted experiments indicating that strength of the compacted submerged granular medium increases gradually due to formation of silicic acid gel at the quartz surfaces in contact. On the other hand, in the studies of pressure solution it was noticed that the presence of clay in the vicinity of contact enhances substantially dissolution of quartz and the ensuing compaction of the sediments (Becker 1995, Bjorkum 1996, Kristiansen et al. 2011). Much more recently AFM and SEM studies of the stressed silica-muscovite contact have shown indeed almost an order of magnitude higher silica dissolution rate (Houseknecht et al. 1987, Meyer et al. 2006).

The proposed research based on the theory that the mechanism through which a granular material stiffens in submerged stressed conditions consists in generation of micro-cracking near the intergranular contact, which constitutes a source of an increasing surface area of inter-phase interface from which dissolution of quartz occurs. This dissolution removes the material from the solid phase, making the material in that zone weaker, and further enhancing the process of micro-cracking (Hueckel et al. 2001). The dissolved mineral may either migrate away in the presence of advective gradients or, in their absence, when local concentrations grow sufficiently, precipitate, polymerize, or gelate.

Recent work by Israelachvili and co-workers at University of California, Santa Barbara showed that difference in electrochemical surface potentials between muscovite mica sheet and silica surfaces is the driving force behind accelerated dissolution of silica. Muscovite as clay particles is present in different quantities in most soils. It is possible that under stressed conditions, silica grains dissolve locally in the presence of muscovite and re-precipitate to other muscovite-free surfaces as silica gel structures, connecting between silica grains and therefore enhancing the macroscopic mechanical properties of sand soil. Verifying this hypothesis of soil aging is another motivation for this research. To investigate the role of muscovite mica in soil aging, both mica powder and mica sheet are incorporated in grain-to-grain crushing experiment as well as macroscopic soil experiment such as consolidation and penetrometer tests. We will explore other materials that also create a difference in electrochemical potentials with silica and test for silica dissolution and re-precipitation rate to see if such behavior occurs between mica and silica only or if it is a more universal phenomenon.

Since soil aging is a multi-scale problem, the microscopic mechanical properties of silica gel structures and its effect on the macroscopic soil properties are investigated separately. Using Atomic Force Microscopy (AFM), pulling experiments are conducted on individual silica polymers to test their tensile strength. Different AFM cantilever tips can be used to map small stressed contact regions between silica grains and reach in to trenches to hook up micro-structures that cannot be studied otherwise. It provides surface mapping in early stages of silica gel growth with nano-meter scale resolution so

to detect extremely small silica polymers. Operating in fluid chamber, the disturbance to structures on grain surfaces by AFM would be minimal.

In the later stages of soil aging in solution, Scanning Electron Microscopy (SEM) provides images of silica structure in the micro-meter scales, giving us a macroscopic picture of silica polymers joining different surfaces. A Pneumatic Cube Crusher is used for this purpose, pressing together two cubes in fluid chamber with a controlled silica content. SEM imaging can obtain the number of polymers generated between cubes per unit area. Once individual silica polymer strength is measured by AFM, such data can help us estimate the total adjoining force the silica polymers can generate per unit area. Macroscopic soil properties such as stiffness can be calculated using the estimated results and compared to literature.

It is thought that when silica grains are in contact in solution with low silica content, silica films instead of protruding gel polymers may grow on silica surfaces in the vicinity of stressed contact region. Excessive drying may destroy this film as water has high surface tension so instead of using SEM imaging, such films can be studied using ZYGO 3D Optical Profiler where films between 1 to 50 microns thick can be detected.

Mesoscopically, the effects of silica gel structures on individual silica sand grains are investigated through a series of grain crushing experiments. Small silica cubes are pressed together by a constant pressure in a liquid chamber containing water with various concentrations of silica ions to obtain SEM images of silica structure growth. The

macroscopic tensile strength of silica gel structures growing between silica grain contacts is measured via a self-designed Spring Cube Crusher as well as a Micro-Strain Analyzer (MSA).

For the Spring Cube Crusher, the cubes are oriented such that the sharp corner of one grain is indenting the flat surface of another cube to simulate real-life scenarios where micro-cracks and debris are generated on sand grains by uneven loading. After an aging period, the device is connected to a load frame and an analytic scale to measure the separation force between the cubes. The force required to separate two silica cubes after weeks of stressed contact in water with various concentrations of silica ions reflects the macroscopic tensile strength of any silica structure growing between the silica cubes.

MSA, on the other hand, is used to investigate aging in soils when flat surfaces of grains are in contact with each other. Two silica cubes will be pressed together by a mounting stage for a period of time in solution. At the end of aging, the staged is mounted to MSA and slowly separated. The force required can be measured and plotted against the gap between two grain surfaces.

In both the Spring Cube Crusher and the MSA methods, different content of mica powder can be added in solution to provide a presence of mica in the vicinity of silica contact region in order to investigate the role that clay particles play in soil aging. Other than mica powder, mica strips can also be inserted between grain contacts to create a silica-mica-silica contact and compare results to silica-silica contact scenarios. Whether electrochemical potential is the driving force of silica dissolution or not, in preliminary

experiments silica polymers have been observed to grow primarily between mica sheet and silica surfaces near contact region. It will be of our interest to find out the mechanism behind such phenomenon and to test for the working range of such mechanism.

Effect of silica microstructures on the macroscopic properties of silica sand, the so called 'soil aging' effect, is investigated by consolidation and penetrometer test. Silica sand in a container is consolidated and then left under a constant pressure for a period of time to allow aging. Stiffness of the sand sample after aging is compared to that before aging to show for difference in soil stiffness. Two containers are to be used for consolidation. A standard container can be used to conduct a standard consolidation test with higher pressure on soil. A larger one with a lid sealed by O-ring can be used so that water sample can be taken from the container at different times to test for silica concentration. Different parameters can be introduced to sand soils for consolidation test, such as muscovite clay content in soil and water content. Electrodes are also present in the container wall to allow for voltage to be applied to the soil sample so to study the effect of electrochemical potentials claimed by Israelachvili and co-workers.

Penetrometer tests can be performed independently on sand soils or during consolidation tests to test hardness of soil during and after aging in the presence of muscovite clay particles. For testing during consolidation test, a special lid is used with a hole drilled in it to provide access for penetrometer.

Other parameters that may influence the dissolution, precipitation, and polymerization of silica, and soil aging in turn, is also investigated, such as salinity, pH, and presence of other ions. In addition, the effect of silica gel structures on grains' capability to rotate is also examined.

The main contribution of the proposed research to the literature lies in the exploration of the mechanisms behind soil aging. By simulating soil contacts on a granular scale in laboratory settings, we hope to isolate and identify the source that generate granular linkages between silica sand and quantify the strength of such linkages. We have postulated that such linkage comes in the form of silica polymer, gel structures, and/or thin films on and between individual grains. Quantifying the strength of such bondage between grains allows us to build a macroscopic model of soil contact that incorporates soil aging effect at different stages. The result would be a much more accurate prediction of in-situ soil properties based on laboratory measurements.

This proposed research will find, for the first time, the mechanical strength of a single silica polymer and its effect on the macroscopic soil properties such as stiffness. The investigation of the effect of mica in the vicinity of stressed silica contact on soil aging will be used to verify a current school of thought that the difference in electrochemical potential between mica and silica is the driving force behind accelerated silica dissolution. It will also identify the possible existence of thin silica films that may develop on silica grain surfaces and find if such structure would provide any bonding force between silica grains in contact.

2. Objectives and tasks

The main objectives of the proposed research are:

- To find the mechanisms behind the time dependent behavior of silica sand aging in the presence of water.
- To verify, through experiments, the hypothesis that silica surface structures, including polymers, gel, and thin films, generated from the local dissolution and re-precipitation of silica is the main reason behind increased soil properties over time.
- To verify a school of thought that different electrochemical potential between surfaces stimulates and accelerates silica dissolution.
- Other parameters that may affect soil aging process, such as water content, salinity, pH, and the presence of other ions will be identified and their effect quantified.
- A model will be developed incorporating all the relevant parameters to estimate and predict in-situ soil properties based on laboratory testing.
- To find the mechanical properties, such as yielding strength, elasticity, and adhesive strength of individual silica polymers growing naturally between silica grains in stressed contact region.
- To quantify the microscopic mechanical adhering force that such silica surface structures can exert to neighboring grains in different conditions. Such data

would then be used to study the macroscopic effect of silica surface structures on soil aging.

- A scaling law to calculate the effect of bonding force such polymers may contribute to macroscopic soil properties will be developed.

This work will be focused on several laboratory simulated aging processes in micro-, meso-, and macro-scale. The main tasks will include:

- To identify microscopic physical, chemical, and mechanical processes during soil aging. The level of pH in water, surface area of grains, as well as grain arrangement may all have effects on how silica is dissolved and precipitated. Sand grains will be saturated in water using different pH and compressed under various pressure and orientation to identify any change in silica precipitation behavior.

- To develop an understanding of mechanisms governing the microscopic processes and growth of silica gel/film structures near the stressed contact. It is known that traces of ions in water such as aluminum affect the dissolution rate of silica. Different imaging and pulling results can be obtained and compared with by introducing different ions into water that saturates the soil in consolidation test and cube crushing experiments.

- To quantify the bonding strength of silica surface structures on silica grains using AFM pulling for individual polymer strength and load frame cube pulling for granular tensile strength. Comparison of such data could provide insight into how much different variables in experiments contribute to the growth of silica structures.

- To verify the effect of mica on soil aging, including silica dissolution and re-precipitation. Recent development discovered mica clay particles stimulating silica dissolution by electrochemical potential difference. Mica powder and sheet will be introduced in cube crushing experiments for SEM imaging and cube pulling tests.
- To plot force vs displacement curves of silica polymers and silica surfaces in contact by measuring weight of cube on scale during load frame cube pulling. Polymer length and gel strength can be measured in force vs displacement curves. This result provides the most direct evidence of the adhesive force between silica cubes provided by silica gel.
- To identify principal variables controlling the aging process at macro-scale. The variables to study are related to water presence, concentration of different ions and particles, pressure in the stressed contact regions, etc.
- To develop a macroscopic model for soil aging and examine its performance using in-situ and laboratory data reported in literature. Single polymer strength and length using AFM pulling and gel structure tensile strength and length using load frame cube pulling will be incorporated together to provide a more complete picture of how much the growth of silica surface structures contribute to soil aging.

3. Literature review

The dissolution of silica in water is very low. According to Krauskopf (1956), which had a very good summary of previous studies of silica dissolution and precipitation, the dissolution of amorphous silica at room temperature was between 100-140 ppm whereas at 90 ˚C its dissolution was raised to 300-380 ppm. He claimed that the solubility of silica remained largely constant between pH 0-9 but increased significantly at pH >9.

However, Iller (1979) offered some slightly different data on solubility of amorphous silica. At room temperature, the solubility of amorphous silica ranged from 70 to more than 150 ppm. Such wide range of solubility was due to many factors such as particle size, state of internal hydration, and the presence of other minerals. The solubility possibly reached a minimum at pH 7-8 but reason behind the slightly higher solubility at lower pH values was unknown.

The hypothesis that the dissolution and precipitation of silica formed silica films between sand grains and created a cementing effect was first brought up by Denisov and Reltov in 1961. They measured the amount of force required to displace a sand grain on quartz or glass plate in water over time. From the results they concluded that "the gradual strengthening of sands in hydraulically placed embankments is due to the formation of silicic acid gel films on the surface of quartz grains".

Mitchell and Solymar (1984) reviewed evidences showing time-dependent stiffening and strengthening of soil in laboratory setting and field observations found in literature prior to 1984. They conducted several tests on soils in the foundation of the Jebba dam in Nigeria, and found that the penetration resistance of saturated clean sand on site increased significantly 11 weeks after blasting. They stated that such time-dependent behaviors cannot be attributed to excess pore pressures or explosive gases and suggested that cement bonding had developed at particle contacts.

Schmertmann (1991) suggested that secondary compression was an important part of soil aging. He demonstrated that the strain of soil ϕ'', a basic soil frictional strength, increased over time for up to 5 weeks using an IDS testing designed by himself. The paper suggested that aging phenomenon in sands was frictional and was due to the sand particles interlocking more effectively in compression, resulting in increases in the frictional component of sand's shear resistance. However, the author did not attempt to study sand grains contact surfaces and pore fluid to rule out possible cementation or bonding of silica materials.

Similar theories were stated by Mesri et al. (1990) and Bowman and Soga (2003). Mesri and co-workers suggested that particles continued rearranging themselves in secondary compression and developed higher frictional resistance to deformation through increase in interlocking of particle surface roughness, and more efficient packing of particles. They proposed an empirical equation they claimed satisfactorily predicted and increase in shear modulus and penetration resistance after primary

consolidation. However, there was no direct evidence to reject the hypothesis that silica precipitates and bonds sand grains together.

Bowman and Soga (2003) conducted a series of triaxial tests on dense granular soils to examine their creep response. It was found that particles rotated and aligned to form tighter clusters and different local void ratios. A model was developed suggesting that frictional slippage of particles contributes to soil aging.

In a series of sand aging experiments conducted by Baxter and Mitchell (2004) using sand, small strain shear modulus was found to have increased over time. Electrical conductivity measurements and mineralogical studies of pore fluid in sand showed that there was dissolution of carbonate and silica. But corresponding small strain shear modulus data did not mirror a higher value, prompting the authors to suggest that dissolution and precipitation of carbonate and silica were not responsible for aging phenomenon. But in this series of experiments, the silica used and tested was in the form of quartz SiO_2, which had significantly lower solubility comparing with amorphous silica. Therefore the amount of silica precipitation in this setting was expected to be lower and slower than if amorphous silica was used.

A numerical model of contact creep in dry, clean sand was developed by Wang et al. (2008) which showed sand particles undergoing a homogenization process under load. The researchers focused on the mechanical process of aging and found that contact creep resulted in a redistribution of contact force, allowing more stable force chains to be established with limited decrease in porosity. Such behaviors caused increases in small-

strain stiffness over time. The model was further developed to study loose and dense sands under various pressures, effect of unloading-reloading cycles, and how fines could increase aging rate due to higher creep in Wang and Tsui (2009).

Joshi et al. (1995), on the other hand, stated that, while the increase in penetration resistance of dry sand was due to secondary compression and rearrangement of grains, precipitation of salts and silica and cementation caused large increases in penetration resistance in saturated state. Test results showed that the increase in penetration resistance in sand grew faster in submerged state than in dry state. Scanning electron microscopy images showed large amount of precipitates bonding between sand grains when soil was aged in a submerged state. It is worth mentioning that the solution used in some of those experiments had a pH of 8.4. While the solubility of amorphous silica above pH 8 was significantly higher, precipitation, however, became more difficult. We are confident that aging phenomenon due to precipitation such as observed by Joshi et al. would be even more pronounced in solutions with lower pH values.

Hu and Hueckel (2007b) argued that in saturated conditions, creep of material under stress was also linked to damages to grains and subsequent mineral dissolution. Mass removal due to dissolution and precipitation at stressed contacts caused chemical softening of material at damage sites and strain hardening at precipitation sites. Creep in this case was interpreted in terms of dissolution and precipitation mechanisms.

Quartz cementation in sandstones in nature was well documented but its origin and the controls on its distribution were still uncertain. Worden and Morad (2000)

identified temperature, pressure, and presence of clay as factors strongly related to quartz cementation. It was interesting that the authors believed clays would inhibit quartz cementation by coating clean substrates that were needed for cementation to grow.

Soulie et al. (2007) used unloaded sand in a water solution saturated with sodium chloride to demonstrate that bonds formed from crystallization of salt at grain contacts enhanced mechanical strength of the soil. Samples of unloaded clean sand were mixed with water saturated with sodium chloride and allowed to evaporate, creating cemented bonds between local grains. In the test times between 15 minutes to 20 hours the macroscopic strength of soil was considerably higher, reflected from the magnitude of force required to rupture the sample.

A model of aging sediment with evolving secondary structure was developed by Hueckel et al. (2001) where the development of secondary structures had four phases. In the first phase, irreversible aging strain was developed during dissolution of soil grains under stress. High concentration gradient formed around grains and precipitation occurred in unstressed solution, which was the second phase. In the third phase, further compression caused failure to primary structure and, possibly, secondary structure that was just formed. In the last phase, during sample retrieval, tension formed between grains and it led to failure of the precipitate.

Hu and Hueckel (2007a) built a three-scale numerical model to study mineral dissolution in stressed grain contact regions with asperities developed from irreversible

damages. At the micro-scale, rigid chemo-plasticity was applied to grain contacts under stress. Mesoscopically, intergranular forces due to precipitation of minerals acted on granular systems. The effect on soil porosity and stiffness is studied at the macro-scale. Cross-scale transfer functions of mass dissolution and precipitation were proposed.

Another factor that affects silica dissolution in stressed granular contacts was the presence of clay (muscovite) particles, as noted by Becker (1995) and Bjorkum (1996). Both papers showed images of muscovite mica grains penetrating deep into neighboring quartz silica grains in sandstones. In addition, Bjorkum claimed that pressure in the silica-mica contact that led to silica dissolution was small, and that silica precipitation was the rate-limiting factor in the quartz cementation process.

More recently, Israelachvili and co-workers at University of California, Santa Barbara discovered that the presence of muscovite mica created a difference in electrochemical potentials between silica contacts and thus induced dissolution of silica. In Meyer et al. (2006), they used a surface forces apparatus to study the thickness of silica layers in contact with mica or other silica contacts found that dissolution of silica was accelerated significantly when there was a difference in electrochemical potential, even between silica-silica contacts. However, no attempt was made to study where the dissolved silica went. But they postulated that fragile silica gel could have grown between contacts. This postulation was later built into an electrochemical corrosion model where they proposed that silica gel grew in pits on quartz grains between mica and quartz contact (Greene et al. 2009).

In another paper by the same group, Kristiansen et al. (2011), they stated that pressure, apart from bringing surfaces into contact, did not have any significant effect on silica dissolution, similar to the statement made by Bjorkum (1996). They also revealed that using solutions with low pH values (<3) would reduce the latency period of silica dissolution.

4. Experimental methods

Five different experimental methods studying effects of silica gel growth in the vicinity of sand grains stressed contacts on soil aging are proposed here. Since soil aging is a multi-scale problem, the proposed experimental methods aim to study silica structures and granular soils on microscopic, mesoscopic, and macroscopic scales. Super-saturated silica solutions are studied for early-stage silica gel growth rate as well as silica polymer tensile strength using Atomic Force Microscopy. Pneumatic grain crushing experiments are conducted to study the growth of silica structures around stressed grain contacts by Scanning Electron Microscopy. Spring cube crushing experiments are conducted to measure the granular bonding force such silica structures exert on neighboring silica grains. Micro-strain testing is performed to measure the same bonding force between silica cubes as an alternative method to spring cube crushing. Finally consolidation tests of sands are performed to study the macroscopic effect of silica structure growth between sand grains on soil aging.

The quartz grains in stressed contact were simulated using amorphous silica cubes (**Figure 1**). Silica is found in both crystalline and amorphous forms in nature. Crystalline silica has long-range orders, involving a tetrahedral coordination of four oxygen atoms around a silica atom. Quartz is by far the most common crystalline form of silica, found in natural sand (Iler 1955). Amorphous silica, on the other hand, does not have any long-range order, but a tetrahedral arrangement between oxygen and silica

atoms still exists locally. The choice of amorphous silica for the test was motivated by two substantial considerations. First, the rate of dissolution of amorphous silica is about one order of magnitude greater than that of its crystalline counterpart (Iler 1955). It appears that this would not only reduce the time of the tests, but also lower the risk of biological contamination. Second, most quartz grains in nature, which are predominantly crystalline, are enveloped by a layer of amorphous quartz (Oelkers et al. 1992). It is believed that such an envelope is generated by silica dissolved from rocks in the presence of mica (muscovite). Hence, for two grains in contact, the indentation of an asperity would penetrate first through the amorphous coating.

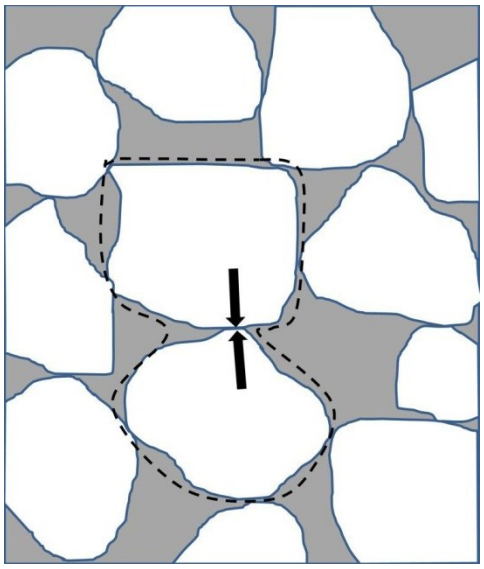

Figure 1: Granular assembly of sand grains

The silica cubes used were made of unpolished amorphous quartz (Prism Research Glass Inc, NC). Quartz sheets were either laser-cut into 1.5 mm x 1.5 mm x 1 mm parallelepipeds, or blade-cut into 30 mm x 30 mm x 30 mm cubes to simulate

common natural sand grain size. The laser processing of cubes had the disadvantage of producing edges that were relatively round, and of irregular length and inclination. This reduced the effectiveness of such edges as indenters.

4.1. Silica gel studies

It is postulated that in stressed contact regions between silica grains the local concentration of silica in solution might exceed the saturation level even though the overall concentration of silica in solution is still below the saturation level. To recreate this scenario under laboratory conditions, since the dissolution rate of silica is extremely low, it would be far more efficient time-wise to have silica grains submerged in a solution that already contains an elevated level of silica ions near the saturation level. Thus when the silica cubes are under stress, a much smaller amount of silica dissolution is needed to bring the local concentration of silica between grains higher than the saturation level and to trigger precipitation of silica.

In the initial stage of this research, conducting experiments with solutions containing silica ion concentration that is higher than the saturation rate also serves as an initial validation of our hypothesis. If initial experiments showed evidence of silica gel growth in solution with higher concentration of silica ions, it is more likely that silica will dissolve in stressed contact region and precipitate to form gel structures between grains.

The solubility of silica is not significantly affected by pH in the range of 2-9, but is considerably greater and proceeds much more rapidly at pH > 9 (Krauskopf 1956).

Therefore for this research, a super-concentrated solution of silica ions was produced and maintained at a very high pH (>10.0) as a mother solution so that silica in the solution would stay in ionized form. From this mother solution, solutions containing different silica ion concentrations can be made at any time at lower pH values.

A 500ml solution of 500 ppm silica ion concentration was made by ionizing 0.696g of amorphous silicic acid powder (H_2SiO_3, Fisher Scientific) in 2ml of 5M NaOH solution and 8ml water with constant stirring at room temperature for 24 hours. All water used in the experiments was purified by a Milli-Q water purification system. After silicic acid powder had been completely ionized, the solution was then diluted with 490ml of water to make the mother solution with 500 ppm silica ion concentration. The pH value of this solution was 10.5. Subsequently, solutions with different silica ion concentration were made from the mother solution by diluting it with water. The pH values of the test solutions were controlled by adding 1M HNO_3 or 1M NaOH.

As an initial validation of our hypothesis, an exploratory experiment was conducted to see if silica gel structure could grow from solution containing high concentration of silica ions. 40ml of solution containing 500 ppm silica ion concentration was taken from the mother solution with its pH value brought down to 5.0. It was stored in a petri dish at room temperature, sealed off by Parafilm to minimize water evaporation. After 2 weeks, a transparent gel was formed at the bottom of the petri dish.

This gel was initially put directly in the Environmental Scanning Electron Microscopy (FEI XL30 ESEM), high vacuum mode for analysis but the evaporation of

water was accelerated in the near vacuum chamber. Since water has very high surface tension the gel structure completely collapsed as water evaporated in vacuum. The hydrogel was crystallized to powder before meaningful images can be taken. Thus subsequent silica hydrogel was treated in Critical Point Dryer (Bal-Tec CPD 030) where water in gel was replaced by liquid CO_2 and evaporated at its supercritical point to change the hydrogel into aerogel while retaining its structure (Schott et al. 2009). The aerogel was then sputter coated with gold for 120 seconds in a Dielectric Sputter System (Kurt Lesker PVD 75) to enhance the resolution of images taken in ESEM.

It was discovered later that silica hydrogels could be kept intact in SEM under Variable Pressure Mode for 10 to 20 minutes before the gel structure was destroyed by drying. Therefore imaging of silica polymers and gel structures growing between silica cubes were all imaged in SEM in this mode.

To study the early growth rate of silica gel in solutions containing elevated silica ions, an Atomic Force Microscopy (Digital Instruments Dimension 3100) with a Veeco TESP k cantilever was used to scan undisturbed solutions with elevated silica ion concentrations. The same cantilever was also used in AFM pulling experiments to study the tensile strength of individual silica polymers growing on silica surfaces in solution.

4.2. Pneumatic grain crushing

To test the hypothesis that silica gel structures grow in the vicinity of stressed contact regions, silica surfaces need to be pressed together under pressure in solution. Such solutions would contain different levels of silica ions and possibly other minerals

to simulate soil pore water. Since sand is a granular material, each grain is in contact with its neighboring grains at different contact angles. A simplified contact model was developed in laboratory, shown in **Figure 2**, where the cube on top was pushed down at a constant force with one of its flat sides facing the edge of the other cube at the bottom.

An apparatus used to simulate sand grains in stressed contact in fluid needs to have the following characteristics. It needs to be able to apply a constant pressure on the grains for up to four weeks; it needs to have a fluid chamber sealed off from the environment to prevent water evaporation over long periods of time; the experiment unit needs to be small enough to fit in a SEM or AFM chamber.

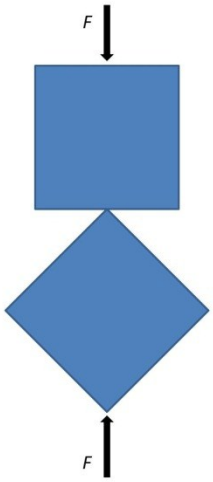

Figure 2: Configuration of silica cubes in cube crushing experiments

Following the above mentioned design principles, a pneumatic cube crushing device was designed by Casey Rubin at Duke University in which two silica cubes were pushed together under pressure in a liquid chamber with the same orientation as described in the laboratory model (Rubin 2009). The configuration of the apparatus and

the fluid chamber unit were shown in **Figure 3** and **Figure 4**. The fluid chamber was made with stainless steel to prevent rusting. The chamber was a separate unit and can be secured to a sturdy steel platform by seven screws around the edges. In the chamber, one cube sat on a raised platform to the left with a corner pointing to the right. The other cube was clamped by a pincer and had a flat side in contact with the left cube's corner.

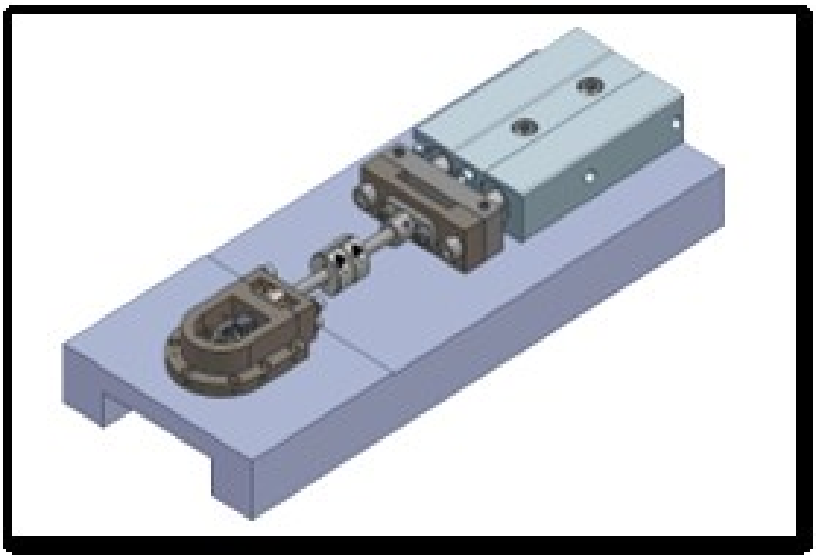

Figure 3: A CAD rendering of the pneumatic cube crushing apparatus

A stainless steel shaft (Misumi, USA) went through an O-ring to prevent water leakage and connected the pincer to a pneumatic actuator (Bimba TB-1625). Around the shaft there was a locking mechanism that secured the shaft in place by screwing tight a collar to the fluid chamber so the whole device can be detached from the pneumatic actuator and brought under an AFM or SEM for imaging. The top of the fluid chamber was sealed with Parafilm and aluminum foil to eliminate water evaporation so that silica ion concentration would not change over time from the decrease of water volume in the

fluid chamber. Pressure was controlled by a pneumatic regulator (Norgren Excelon Pro B92G). The area of interest would be the contact region between two cubes in the liquid chamber. The chamber was compatible for SEM imaging and AFM imaging and pulling in our laboratory.

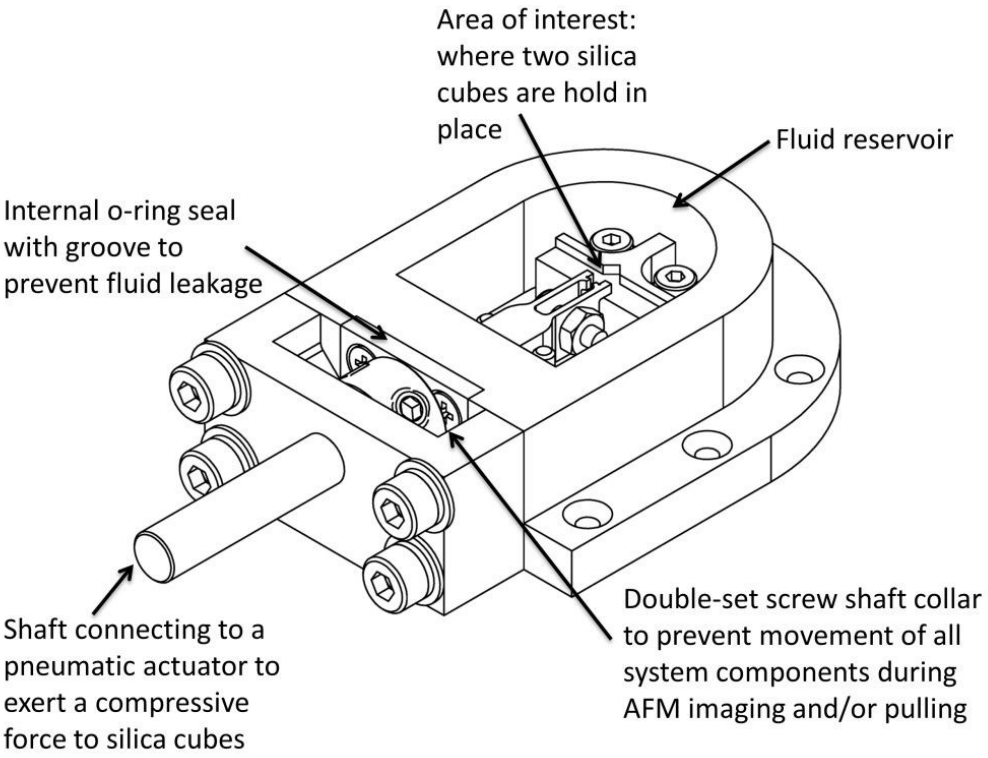

Figure 4: Detailed configuration of the fluid chamber in pneumatic cube crushing apparatus (Rubin 2009)

To perform a pneumatic grain crushing test, two amorphous silica cubes with 1 mm x 1 mm x 1.5 mm dimensions were secured in the pincer and the platform. The shaft was then connected to the pneumatic actuator and pressure slowly turned up to 17 psi. The fluid chamber was then filled with solution containing a certain level of silica ions and sealed by Parafilm. At the end of the testing period which typically lasts two to

three weeks, pressure from the actuator was slowly turned off. The solution was then drained from the chamber and the chamber unit was then unfastened from the platform and transported to SEM or AFM for imaging.

To investigate how the presence of clay might enhance silica gel structure growth between stressed silica contacts, muscovite mica was introduced in some experiments via two ways. One way was to insert a mica sheet between silica cubes before the cubes were pressed together so a silica-mica-silica contact was created. The other way was to mix mica powder in the solution that was used to fill the liquid chamber so that tiny mica particles were suspending in solution and around silica stressed contacts.

4.3. Spring cube crushing

After studying the tensile strength of silica polymers, and silica gel growth in the vicinity of stressed silica contacts, the next step in the research was to study how the growth of silica gel affects the bonding between sand grains. Based on our hypothesis, the growth of silica gel between stressed silica cube contacts must contribute a significant portion of bonding forces between silica grains to make soil exhibits aging phenomena such as increased compressibility over time.

An apparatus needs to be built where silica grains can be pressed together for two to three weeks under constant pressure in solution and then pulled apart at very slow speed while the pulling force was recorded. As the two cubes were slowly separated, any gel structures attached to both cubes would exert a force to counter the pulling force applied to the two cubes. Such sudden changes of force would be reflected

on the mass reading from the analytic scale. This way the bonding force due to the growth of silica gel between silica cube contacts can be recorded.

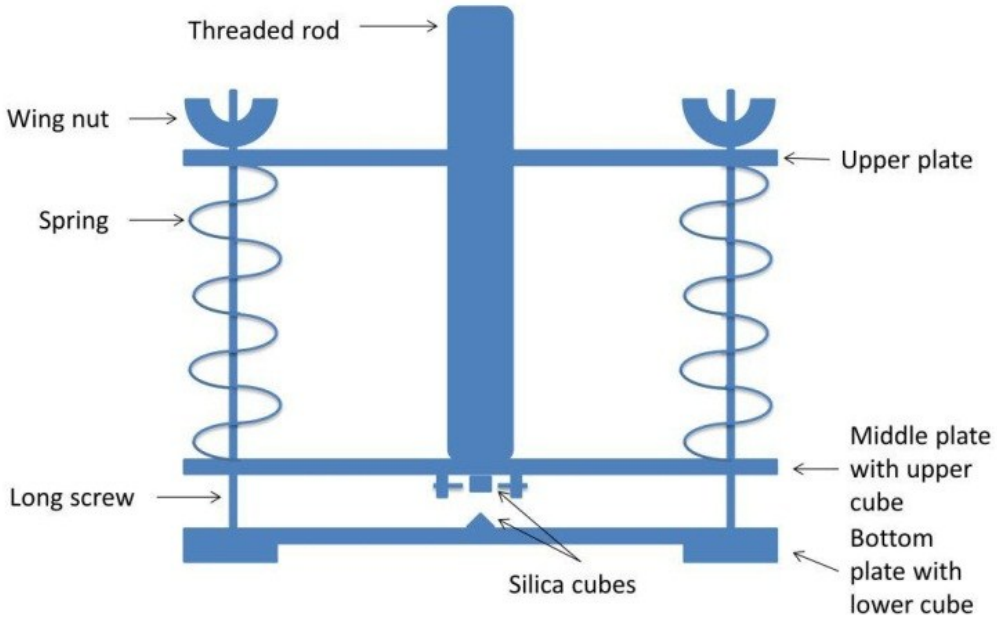

Figure 5: Schematics of spring cube crushing apparatus

A Spring Cube Crusher was thus designed, as shown in **Figure 5**. Two silica cubes were secured between the bottom and the middle metal plates. One cube sat on the bottom plate with an edge pointing upward. The other cube was fastened by screws on to the middle plate with a flat face facing downward. Four springs were placed between the middle and the top metal plates. Four long screws went through all three metal plates, securing them together with wing nuts on top. As the wing nuts were tightened, the springs were compressed, therefore exerting a constant downward force on the middle plate which held the two silica cubes together under constant pressure. The amount of force exerted by the springs can be calculated by multiplying the distance

of compression (converted from the number of turns applied to the wing nuts) and the spring constant. The metal plates were made of aluminum to minimize weight and prevent rusting. All screws were made of stainless steel.

To start a spring crushing experiment, assemble the apparatus and place two amorphous silica cubes with dimensions 3 mm x 3 mm x 3 mm on the bottom and middle plates. After a desired amount of pressure is applied to the cubes by tightening the wing nuts, the device is placed in a plastic container with solution containing a certain level of silica ions. Make sure the solution level is higher than the middle plate so both cubes are submerged in solution. Place the container in an air-tight box together with a fully soaked sponge to minimize water evaporation from the solution.

After two to three weeks of aging, the device is removed from the box and attached to a load frame (benchtop universal testing machine by Tinius Olsen, S-H50KS), as shown in **Figure 6**. Operate the load frame to make the apparatus sits firmly on an analytic scale placed beneath the load frame.

Remove the top plate and springs from the apparatus so that the silica cubes are no longer pressed together by the springs. Instead, the long threaded rod attached to the load frame pushes the apparatus firmly on the scale. Then slowly raise the middle plate up from the bottom plate so to separate the two cubes. Depending on the test conditions the operating speed of the load frame is typically set at 16.7 nm/s (0.001 mm/min), which is the minimum operating speed. As the top cube is pulled away from the bottom cube, adhesive forces applied to the cubes by any silica gel structures growing between the

two cubes would be reflected on the reading on the analytic scale. When a silica polymer attached to both cubes is being stretched, it would exert an uplifting force on the silica cube, resulting in a sudden reduction in reading on the scale. As the cubes are pulled further apart, such polymers would eventually break and the reading on the scale would increase slightly to reflect such action. A force-extension curve can be plotted from recording the analytic scale reading. Such data can provide an estimate to the size and strength of silica gels growing between the two silica cubes.

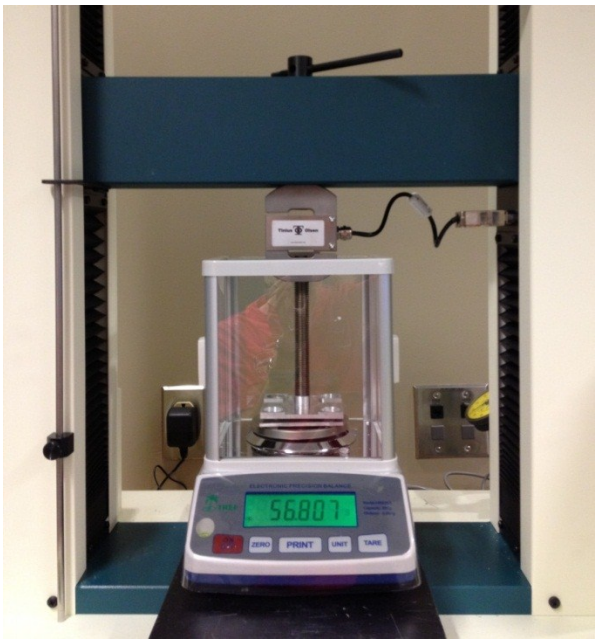

Figure 6: Spring cube crushing apparatus attached to load frame and analytic scale

To investigate the possibility that the presence of clay may induce silica dissolution and thus indirectly increase the polymerization process of silica in stressed contacts, muscovite clay was introduced in the experiments much the same way as it

was done in the pneumatic grain crushing experiments. Either mica sheet was inserted between silica cubes, or mica powder was mixed in the solution bath.

The Spring Cube Crusher had two problems. Firstly, the analytic scale picked up vibrations and air flows from the room it was in which caused fluctuations in reading. It was hard to filter out the noise in the data and thus lowered the confidence level of any estimation to silica gel size and strength. Secondly, all measurement data had to be recorded by hand and the process was very time-consuming. Because mass on the scale changed continuously as the cubes were pulled apart, a video camera was used to record measurement data from the analytic scale. After the experiment was finished, the researcher had to playback the video and manually recorded the mass reading every second.

4.4. Micro-strain testing

To overcome the two shortcomings of the spring cube crushing device, as well as to increase the number of tests that can be performed at the same time, a simple micro-strain testing device was made. This device had to be used in combination with a Micro-Strain Analyzer (TA Instruments RSA III).

The micro-strain testing device comprised of two thin beams with threaded holes at both ends, and two brackets that fitted on the Micro-Strain Analyzer. The beams were made from aluminum to minimize weight and prevent rusting.

Two amorphous silica cubes with dimensions 3 mm x 3 mm x 3 mm were secured by the brackets on the Micro-Strain Analyzer. The two cubes were moved

together by the machine until they just touched each other with no force exerting on either cube. Then the two aluminum beams were sliced into the brackets with the two cubes sandwiched between. Two screws were then fastened on the beams so that they held the two cubes rigidly together. Then the brackets from the Micro-Strain Analyzer were removed and the held-together cubes were transported into an air-tight solution bath containing elevated level of silica ions for two to three weeks.

After the aging period was completed, the cubes were mounted back to the Micro-Strain Analyzer. The aluminum beams were removed after the cubes were securely held by brackets. Then the top cube was slowly raised up while the machine recorded the amount of force required to separate the two cubes. A force-extension curve similar to the one from spring cube crushing experiments could be obtained. Such curves could help estimate the bonding force between the cubes due to the growth of silica structures between them. To investigate the effect of muscovite mica on the growth of silica gel structures between silica cubes, thin mica sheet was inserted between cubes before contact was made in some experiments.

4.5. Consolidation testing

Consolidation tests will be conducted to investigate how aging phenomenon in sand would affect soil's compressibility. Ottawa ASTM Graded Sand will be washed in distilled water, dried in oven, and mixed with mica powder. Distilled water is then added to the mixture and the soil will be compacted to achieve a water content as close to 100% as possible. Then the soil will be loaded in a consolidation machine and the

weight on the consolidation machine will be doubled every 24 hours for seven days until the pressure on the soil reaches 400 kPa. An automated odometer system is used to measure and record the displacement of the metal lid on the consolidation machine. At the end of the 7^{th} day, 10% more weight will be added and the system is allowed to age for two weeks. Displacement-time graph can be plotted on semi-log-scale and compared to literature to identify how much increased compressibility of soil is due to aging phenomenon.

A control test was performed in the lab using Ottawa ASTM Graded Sand without any mica powder mixture.

5. Preliminary results

5.1. Growth of silica gel in solution

Samples of 300 ppm silica ion concentration solution with pH value of 5.0 were taken from a sealed plastic test tube 1 week and 2 weeks after the experiment started at day 0, and imaged in AFM fluid imaging mode. To maintain the concentration of silica ions in the solution, the test tube was filled fully to minimize the air space between the liquid surface and lid in order to minimize evaporation. **Figure 7** and **Figure 8** show the growth of silica structures at day 8 and day 15 respectively.

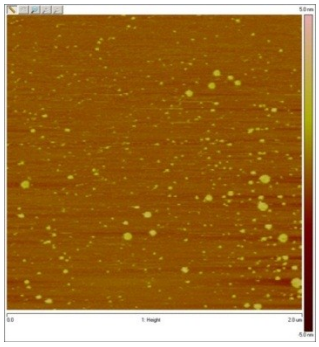

Figure 7: AFM image of 300 ppm Si ion concentration solution after 7 days

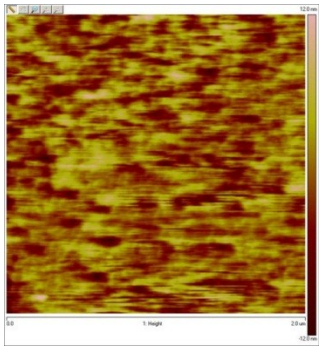

Figure 8: AFM image of 300 ppm Si ion concentration solution after 15 days

At day 8 (Figure 7), many silica seeds with diameter of the order of 10s of nanometers appear in the solution, represented as bright spots on the mica substrate; at day 15 (Figure 8), an interconnected network of gel appears in the solution, but the height of the structure was only around 30 nm, and each polymer width was at least one magnitude less than 1 μm. nevertheless, the density of such structures and their interconnectivity is quite impressive. With a scanning area of only 2 μm x 2 μm, the AFM is not able to give an estimate to the size of the complete gel structure at this stage.

Figure 9 shows the growth of silica structures at day 8 in 180 ppm silica ion concentration solution. Silica seeds similar to those in 300 ppm solution are seen in the solution but it is clear that these seeds are smaller in diameter compared with the seeds seen at the same growth stage in 300 ppm solution. The one big dot in the image may be a dust particle from the environment.

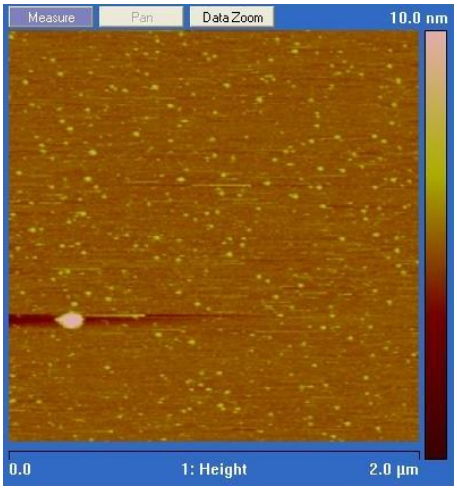

Figure 9: AFM image of 180 ppm Si ion concentration solution after 7 days

More solutions were prepared at lower silica ion concentrations but no silica gel structures were seen in the solution. **Figure 10** shows a typical result from a 150 ppm silica ion concentration solution after 2 weeks. The image shows a clean substrate surface with no traces of silica gel seeds or gel structures.

As gel grew larger in higher concentration solutions, it soon exceeded the capability limit of AFM fluid imaging since the size of an AFM cantilever was only a few microns. When a visible layer of silica gel covered the bottom of a petri dish containing 500 ppm silica ion concentration solution, the gel was scooped up and made into aerogel form in a Critical Point Dryer and then sputter coated with a thin layer of gold. **Figure 11** shows a piece of hydrogel prepared this way. Using 5000x magnification the internal structure of the gel is revealed to consist of a network of thin polymers and interconnected chambers, as shown in **Figure 12**. The thickness of such polymers is in the order of 10 nm.

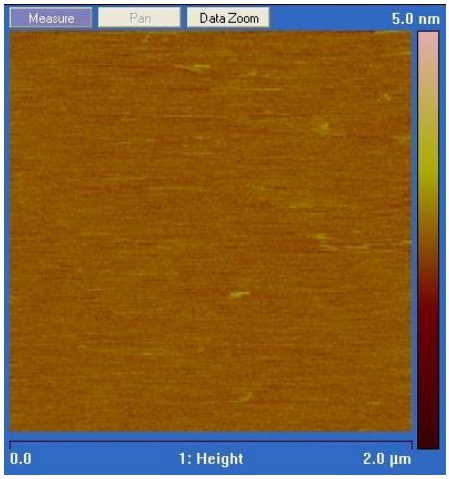

Figure 10: AFM image of 150 ppm Si ion concentration solution after 2 weeks

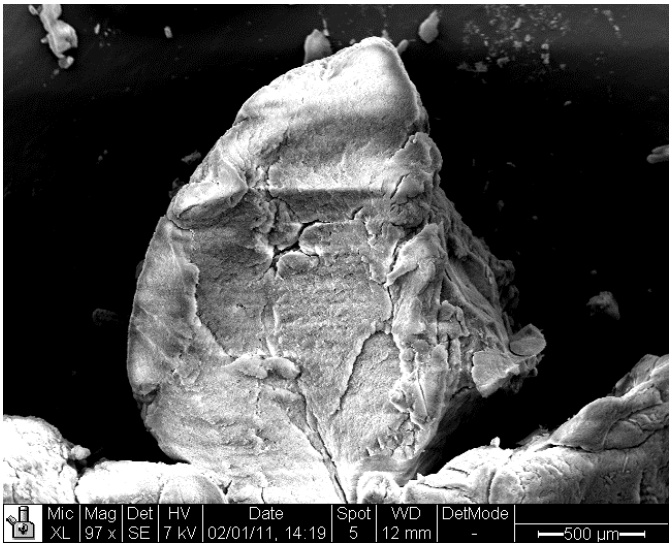

Figure 11: Silica aerogel, gold coated, magnification x97

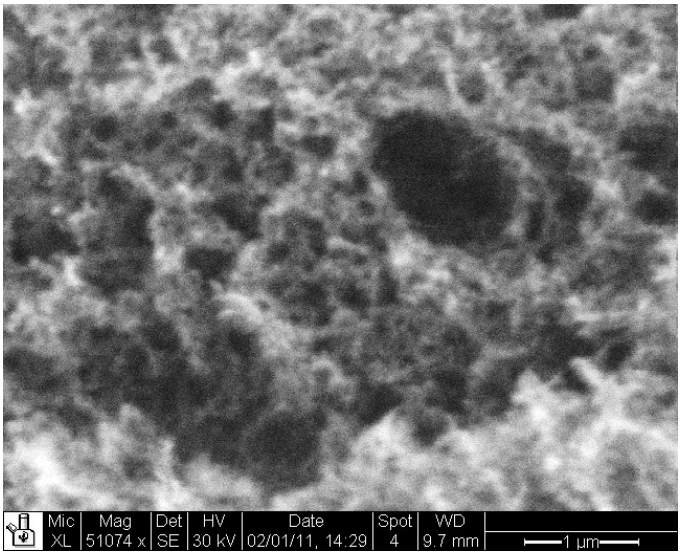

Figure 12: Internal structures of silica aerogel. Magnification x5174

5.2. Growth of silica gel near stressed contacts

A series of tests to assess the growth rate of silica polymer were conducted at different elevated concentrations of silica ions in the environmental solution. The rationale for using an initial elevated concentration (Rubin 2009), after finding a

concentration high enough to induce polymerization or gelation, is to bring the concentration somewhat below that level. Then allow some time for sufficient dissolution from the damaged material to bring the solution to the concentration level at which silica will polymerize. The concentration of silica in the pore solution may be much higher locally and instantaneously near the asperities and stressed and dissolving contacts than the average pore water concentration.

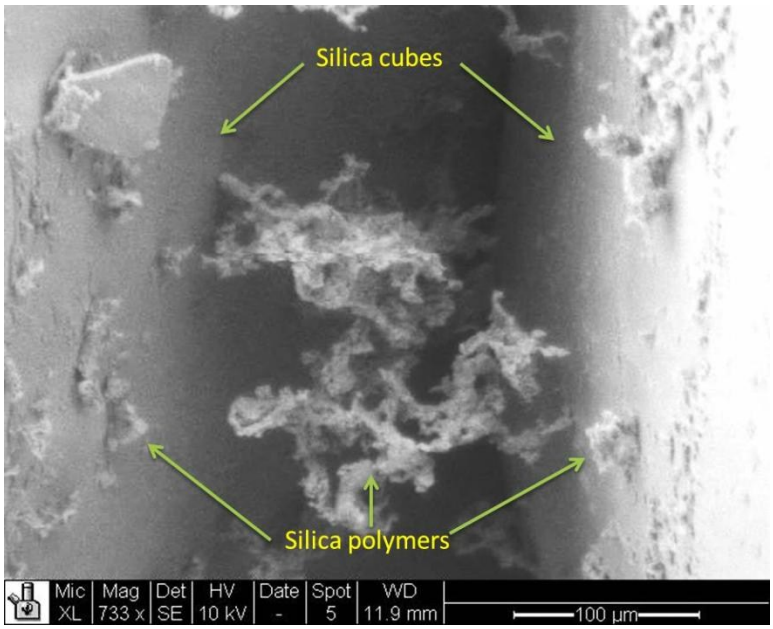

Figure 13: Silica polymers near contact between two silica cubes in 500 ppm Si ion concentration pH 5.0 solution after 3 weeks

In 500 ppm Si ion concentration pH 5.0 solution, after two silica cubes were pressed against each other for 3 weeks, polymers were observed on the surfaces of both cubes in SEM (**Figure 13**). Some of the polymers connected to both cubes near the contact regions were up to several hundred micrometers long. A composition analysis of such polymers using energy dispersive X-ray spectrometer (EDS) showed that the

structures were mostly silica, with minor traces of chlorine, chromium, iron, sodium, and carbon elements (**Figure 14**). These elements were likely originated from the stainless steel liquid chamber and solution residues. The minimal amount of carbon in the sample may come from dust in the environment. It proved that the structure was not of biological origin, because otherwise carbon would be a dominant element in the polymer structure.

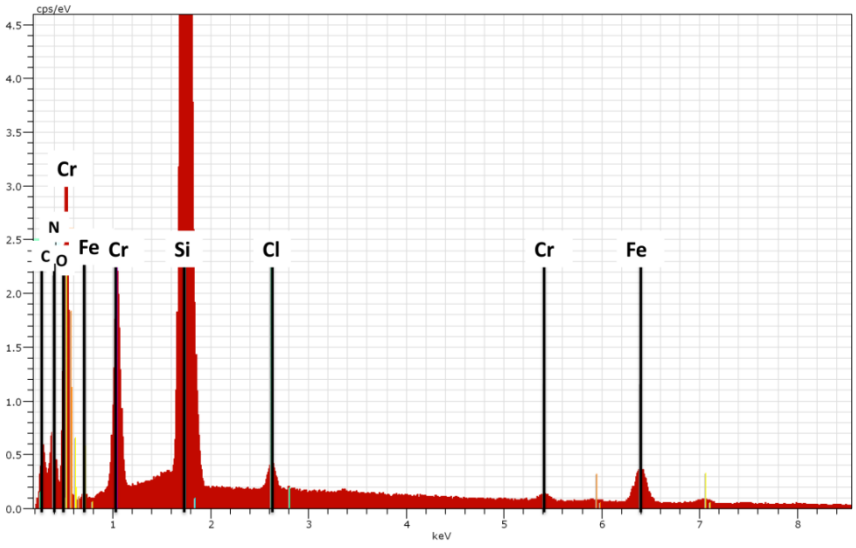

Figure 14: Energy Dispersive X-ray Spectrometer composition analysis of structures in Figure 13

Another experiment was conducted in the same conditions but the cubes were allowed to age for 4 weeks. SEM images showed a network of silica gel growing around a silica cube (**Figure 15**). The fibers that were the walls of interconnecting chambers were much thicker comparing with the fibers from the three-week aging experiment.

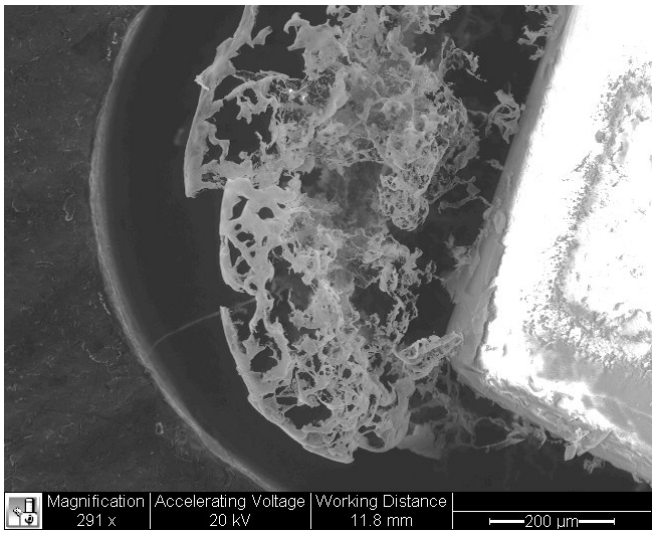

Figure 15: Silica gel growth near silica cube aged for 4 weeks in 500 ppm Si ion concentration pH 5.0 solution

In 300 ppm Si ion concentration pH 5.0 solution, a similar experiment with the same set-up was conducted and aged for 2 weeks. The results showed extensive silica deposits with size of the order of 10 μm developed near the asperities as a result of compression (**Figure 16**). The experiment was repeated with the pneumatic actuator applying a lower pressure (120 kPa) to the cubes. It was found that no microcracks had developed on either cube, no silica polymer deposits were found anywhere in the liquid chamber (**Figure 17**).

In 200 ppm Si ion concentration solution with pH 2.5, two silica cubes were compressed together and aged for 3 weeks. SEM images showed an extensive silica gel structure growing around the contact region between two silica cubes (**Figure 18**). Interestingly, some larger gel structures were seen connected to the cube surfaces by very thin fibers as shown in **Figure 19**.

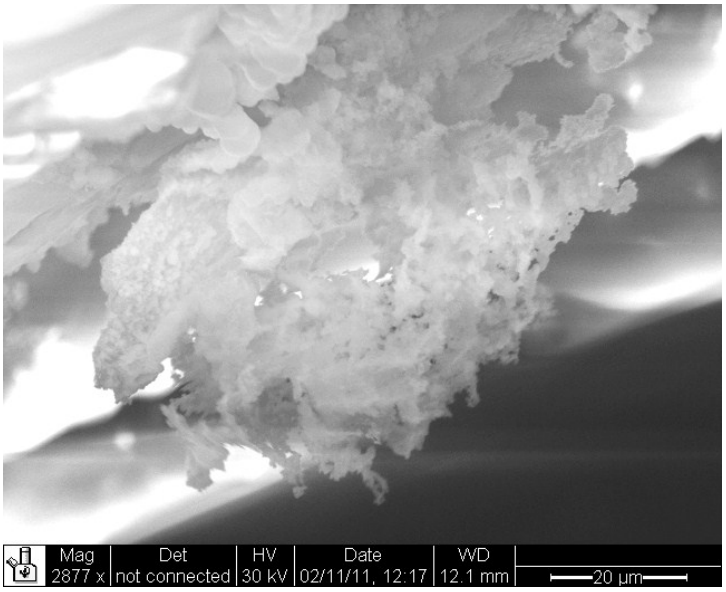

Figure 16: Silica deposits in silica cube crack after 2 weeks aging in 300 ppm Si ion concentration pH 5.0 solution

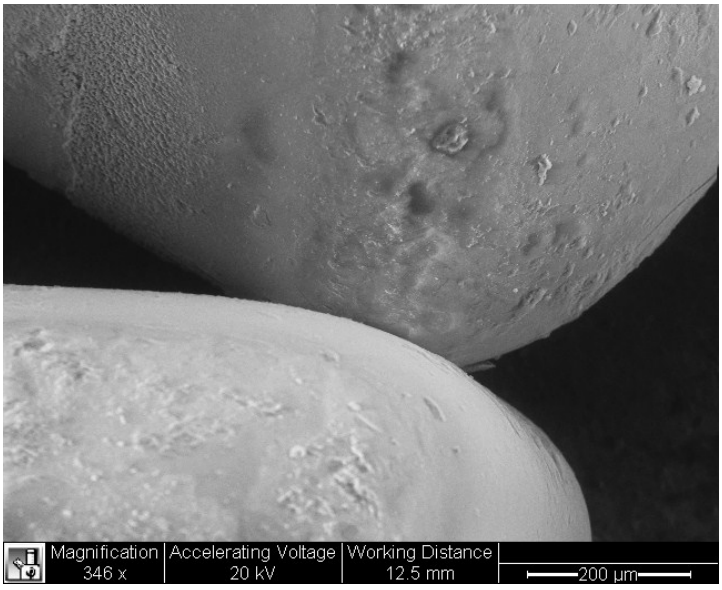

Figure 17: Clean cube surfaces after 2 weeks aging in 300 ppm Si ion concentration pH 5.0 solution

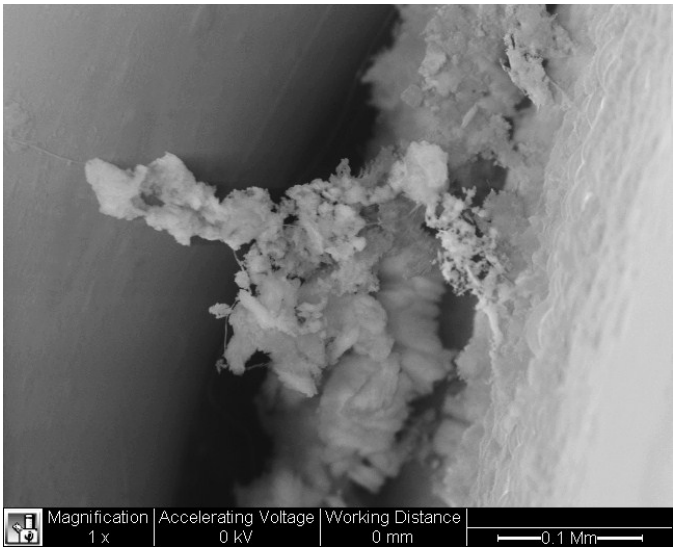

Figure 18: Silica gel growing on cube surfaces after 3 weeks aging in 200 ppm Si ion concentration pH 2.5 solution

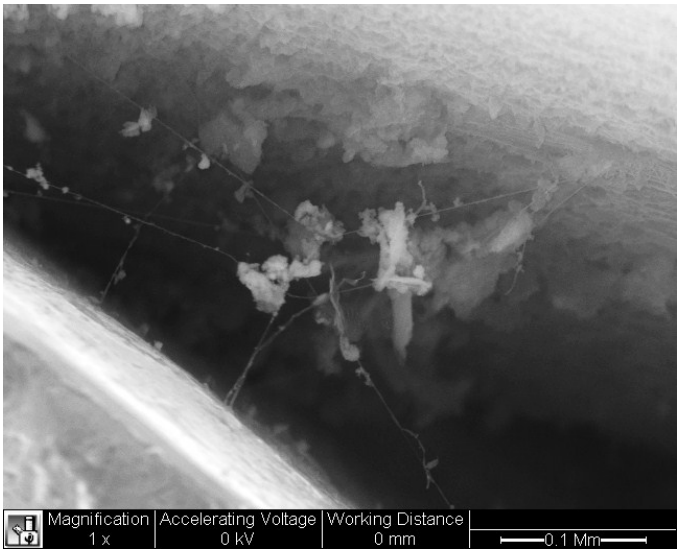

Figure 19: Thin polymers connecting silica gel to cube surface, seen in 200 ppm Si ion concentration pH 2.5 solution after 3 weeks aging

In 90 ppm Si ion concentration pH 5.0 solution, polymers a few micrometers in length were found between a cube's main body and a piece of silica debris that was

chipped off from compression after aging for 3 weeks(**Figure 20**). No extensive silica deposits were found otherwise.

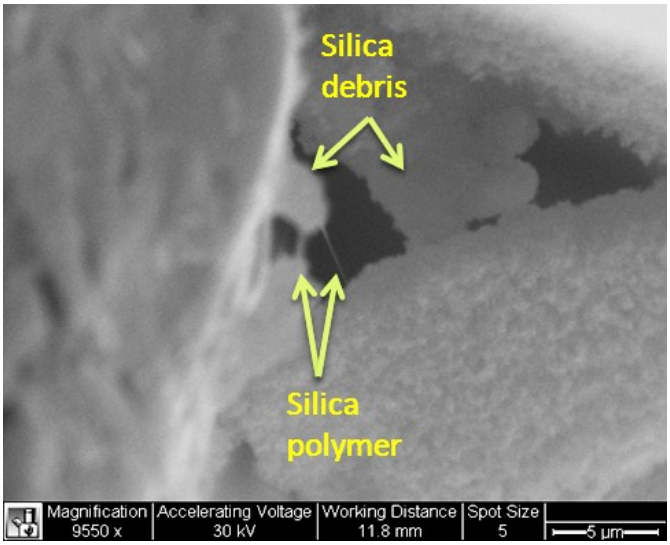

Figure 20: Silica polymer growth in 90 ppm Si ion concentration pH 5.0 solution after 3 weeks aging

5.3. Tensile strength of silica polymers

AFM pulling experiments were conducted on silica cube surfaces to measure the tensile strength of silica polymers growing there. An AFM cantilever tip was slowly lowered in solution until it touched the cube surface, at which point it was slowly raised up from the surface. If the tip was in contact with any silica polymers on the surface, surface tension would make the polymer attached to the cantilever. As the cantilever was pulled away from the surface, the polymer was stretched between surface and cantilever until the polymer was broken. The deflection on the cantilever was recorded and, knowing the spring constant of the cantilever, the tensile strength of the polymer could be estimated.

Undisturbed (not loaded) silica cubes left in solutions with Si ion concentrations ranging between 130 ppm and 210 ppm and pH 5.0 for 2 weeks were put in AFM, and pulling experiments in water were conducted on those cube surfaces. On cube surfaces in the 210 ppm solution, distinctive kinks were consistently captured on the force curves (**Figure 21**).

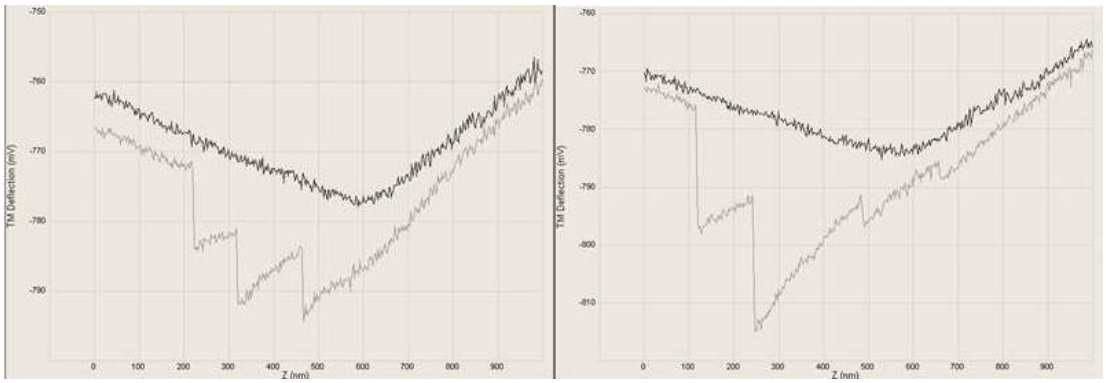

Figure 21: AFM force curves on cube surface in 210 ppm Si ion concentration pH 5.0 solution for 2 weeks

The black curve represented the force curve as the cantilever tip approached the surface. The grey curve represented the force curve as the cantilever pulled away from the surface. The vertical distance between the two curves represented the additional force required for the cantilever to overcome surface tension, short-range forces, and any potential polymers connecting the tip to the surface. This force was calculated by multiplying the distance with cantilever deflection sensitivity (30 nm/mV) and spring constant (0.74 nN/nm). The peaks shown in (**Figure 21**) possibly indicated instances when polymer segments were broken as the cantilever was pulling away. Therefore the vertical distance between a peak to the approaching force curve can be converted to

force magnitude for an estimation of polymer strength. In Figure 21 the average vertical distance from a peak to the approaching curve was about 15 mV, which converted to 330 nN. **Figure 22** showed a testing cycle with smooth approaching and withdrawing force curves, indicating that no polymers were picked up and thus can be used as a set of control data. Small jumps were recorded when the tip was about the leave the cube surfaces, most probably as a result of surface tension. Such step-like force patterns were not obtained on cube surfaces in solutions with 130 ppm or 170 ppm Si ion concentrations.

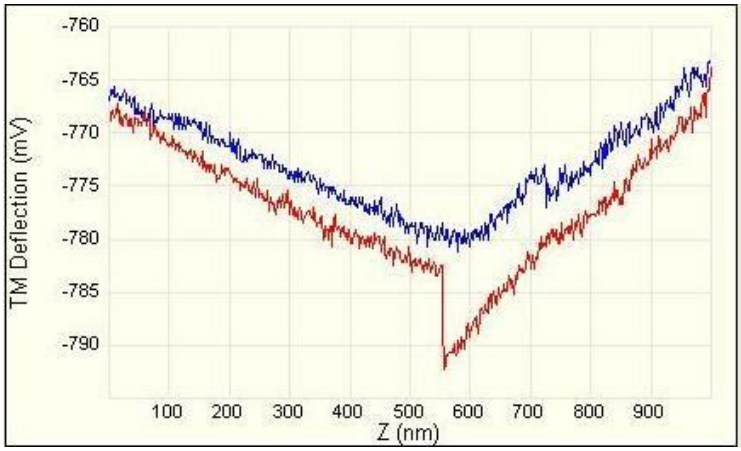

Figure 22: AFM force curve on silica cube surface with no polymers picked up

5.4. Strength of silica gel between grains

After measuring the tensile strength of individual silica polymers growing on silica surfaces in solutions containing Si ions, the next step was to measure the amount of bonding force silica gels can exert between two silica cubes. Spring cube crusher devices were used for this purpose. Force between cubes at any time during the experiment was calculated by taking the difference of analytic scale reading at that time

and the final reading on the scale when the cubes were well separated. Any such mass difference was a result of interactions between the two silica cubes in motion and was converted to force.

Figure 23 showed a curve of adhesive tensile force between cubes against displacement between cubes at the end of a three-week compression test in spring cube crusher in solution with 500 ppm Si ion concentration pH 5.0 solution. The total adhesive force between cubes peaked at 15.5 mN before slowly reducing as cubes became further apart.

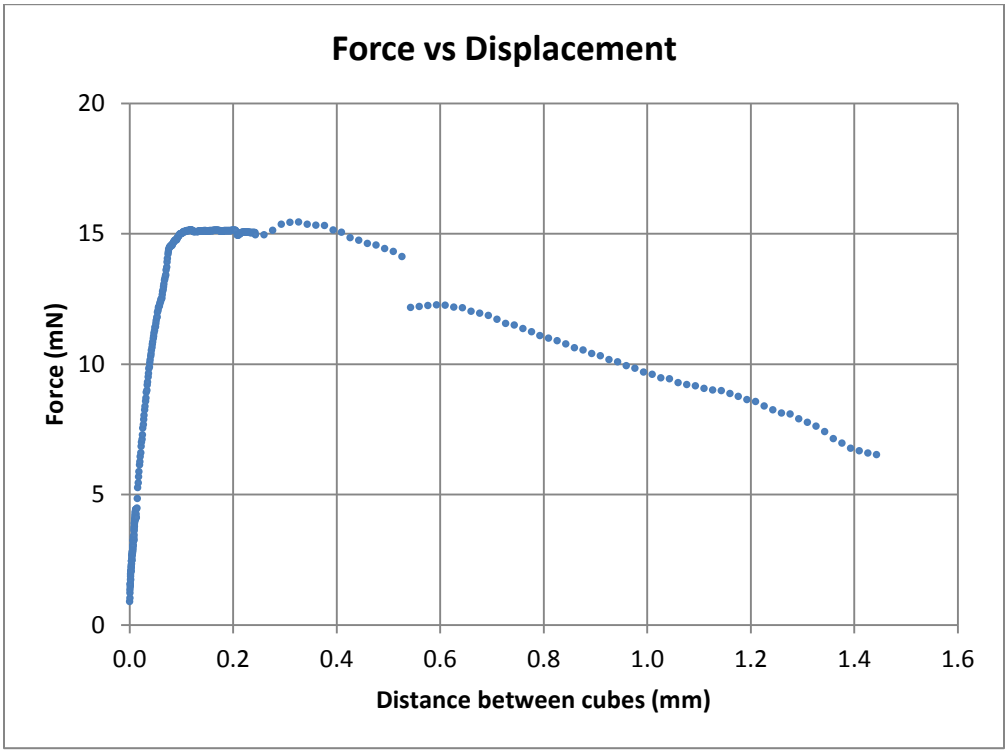

Figure 23: Adhesive force against cube displacement for cubes in 500 Si ppm pH 5.0 solution for 3 weeks

The peak region of the curve was zoomed in in **Figure 24** to show some subtle yet key features of this curve. The force curve reached an initial peak of 15.15 mN at 0.1172 mm extension. Five sudden drops in force were recorded starting at 0.1188 mm, 0.1447 mm, 0.1713 mm, 0.2030 mm, and 0.2395 mm respectively. Between the first and the fourth drop in force, the force curve had a slightly positive average gradient, whereas between the fourth and the final force drop, the gradient turned slightly negative. The first peak in force (15.15 mN) was not exceeded until after the fifth drop in force, after which the curve rose to its second peak of 15.45 mN at 0.3261 mm. It then started decreasing all the way back towards zero.

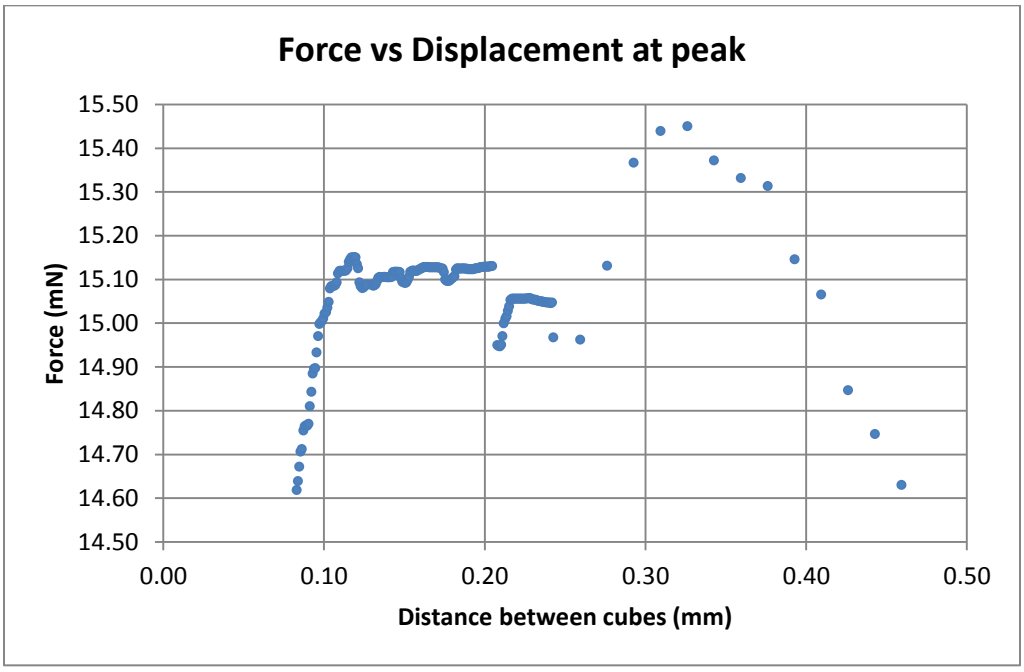

Figure 24: Force-Displacement curve around the peak

The magnitude of the five force drops were 66.7 μN, 22.6 μN, 27.5 μN, 180 μN, and 79.5 μN respectively. The horizontal distances between these drops were 25.8 μm,

26.7 μm, 32.3 μm, and 35.0 μm respectively. We believe the force magnitudes of the five kinks on the curve were indicative of tensile strength of silica polymer clusters or gels connected between the two cubes. The horizontal distances between kinks indicated the overall length of such gel structures at full stretch.

A control experiment was conducted where two clean silica cubes were compressed together in spring cube crusher in water and immediately followed by a pulling experiment. The resulting force-extension curve was shown in **Figure 25**. There was a single peak in the force close to contact point before it started decreasing. The magnitude of the force peak was 6.7 mN. No other force plateau or sudden changes in magnitude were observed.

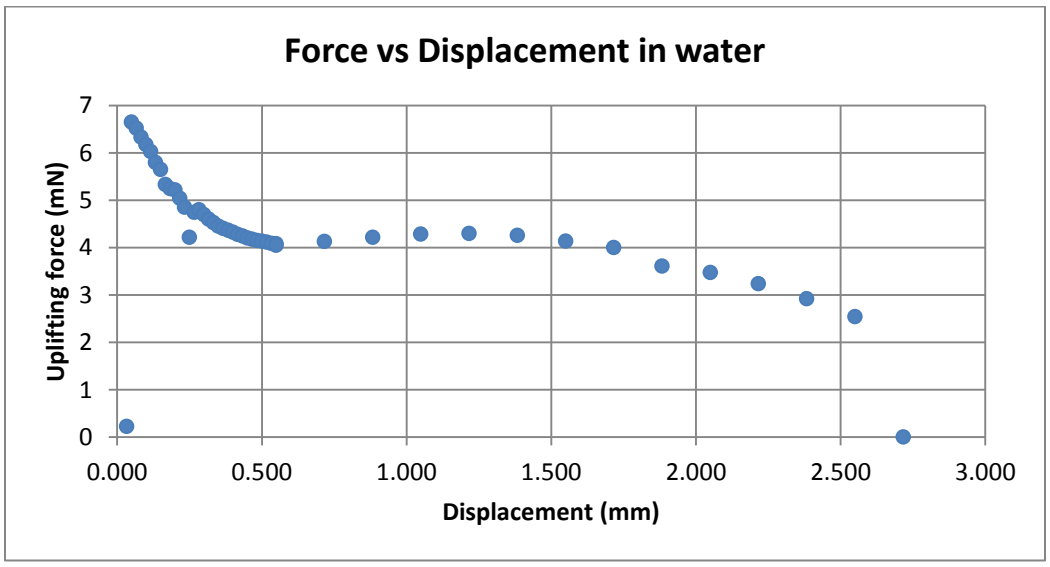

Figure 25: Force-Displacement curve for control experiment

A second cube crushing test was conducted in the same pH 5.0 500 ppm Si ion concentration solution but the cubes were allowed to age for 4 weeks in compression.

The resulting force-extension curve was shown in **Figure 26**. The curve was relatively smooth with a positive gradient. No force plateau or kinks were observed. Since adhesive forces between cubes exerted from stretching inter-granular silica gel structures would result in an increase in force magnitude, the difference in force magnitude between each two consecutive data point was taken. The result was shown in **Figure 27**. It was clear that the highest net decreases in mass occurred at the beginning of the test when cubes were in close proximity. The largest increase in force, 0.785 mN, occurred at a displacement of 25.8 microns. As the cubes were separated further apart, magnitudes of force increase gradually became smaller.

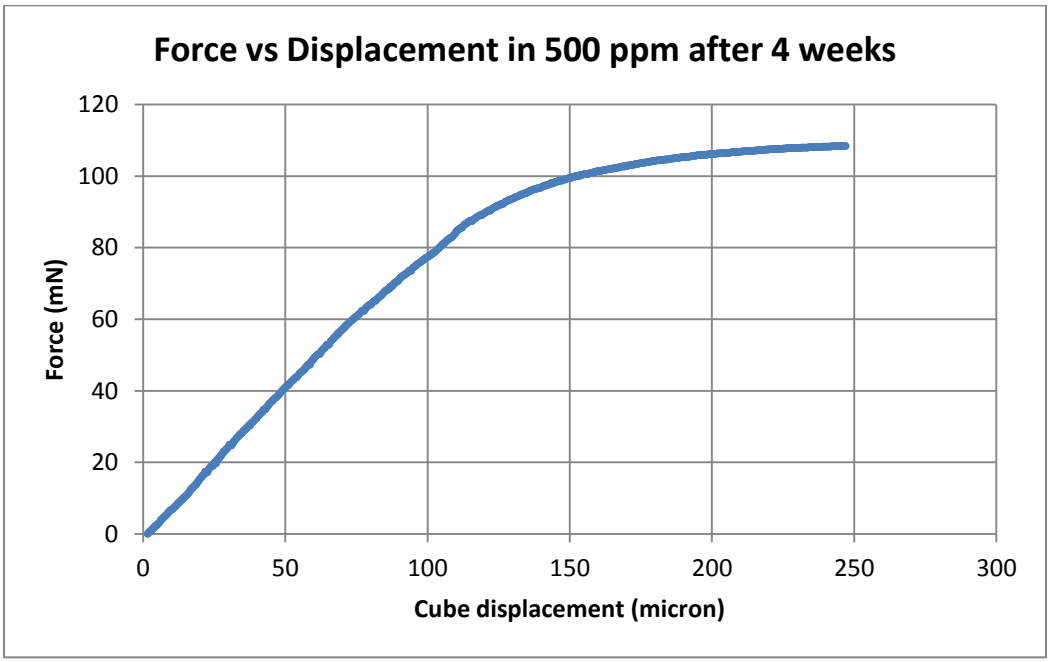

Figure 26: Another Force-Displacement curve in 500 ppm solution

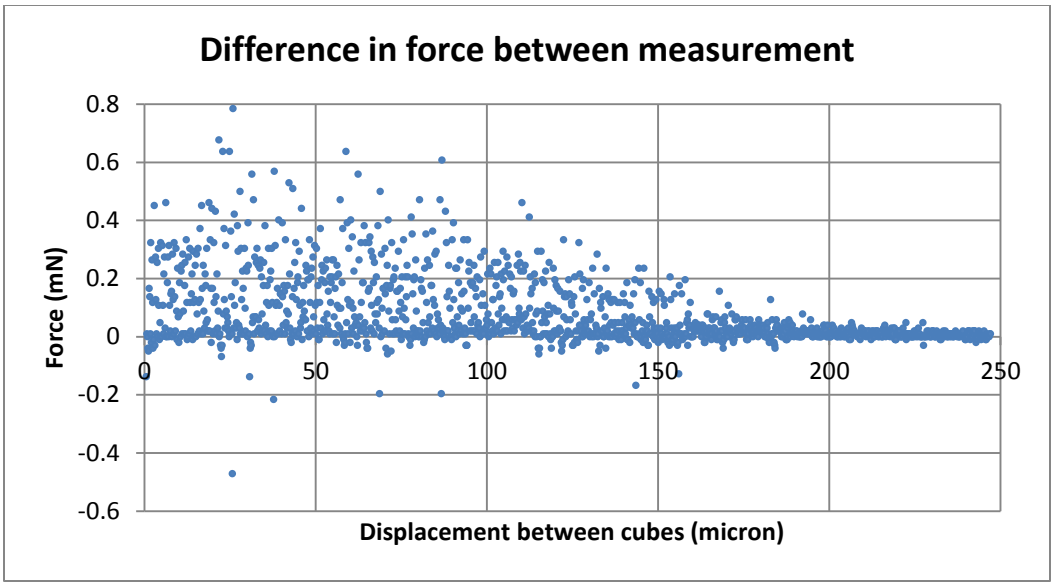

Figure 27: Difference in force magnitude between consecutive measurements

Two more cube crushing experiment was conducted where the cubes were submerged in solution containing 300 ppm Si ion concentration and aged for 3 weeks. In the first test the pH value of the solution was 2.7. The force-extension curve had an overall positive gradient, as shown in **Figure 28**. A peculiar force pattern was observed when zooming in to the curve, shown in **Figure 29**. Magnitude of force would change continuously followed by a sudden jump and then the pattern repeated. Force magnitude for each jump was in the order of 0.1 mN. The data was then filtered using the same method mentioned previously (**Figure 30**). The decreases in force were fairly random. The largest drop in force was 0.824 mN, occurring at a displacement of 10.55 microns.

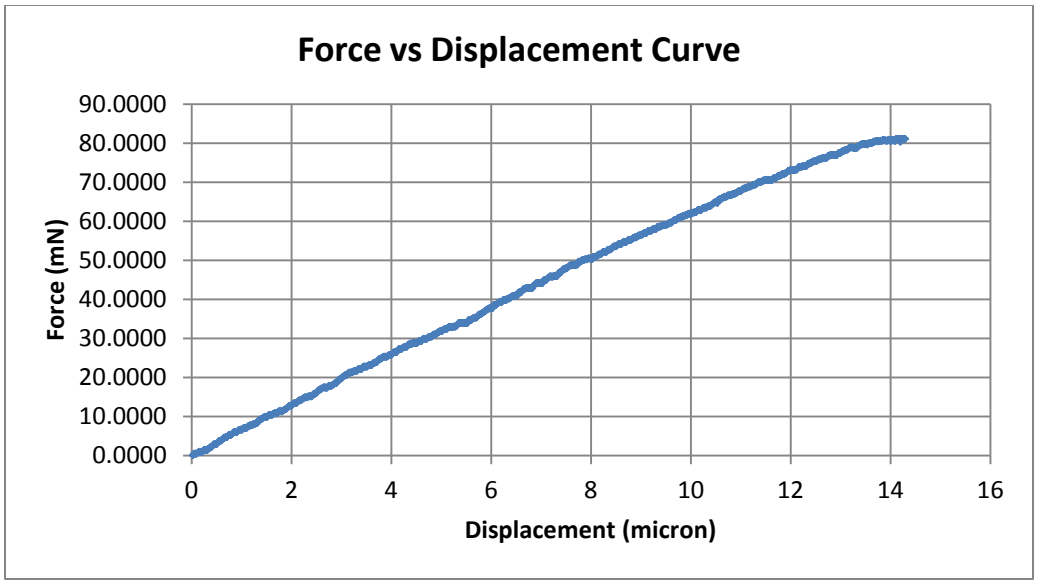

Figure 28: Force-displacement curve, 300 Si ppm, pH 2.7, 3 weeks

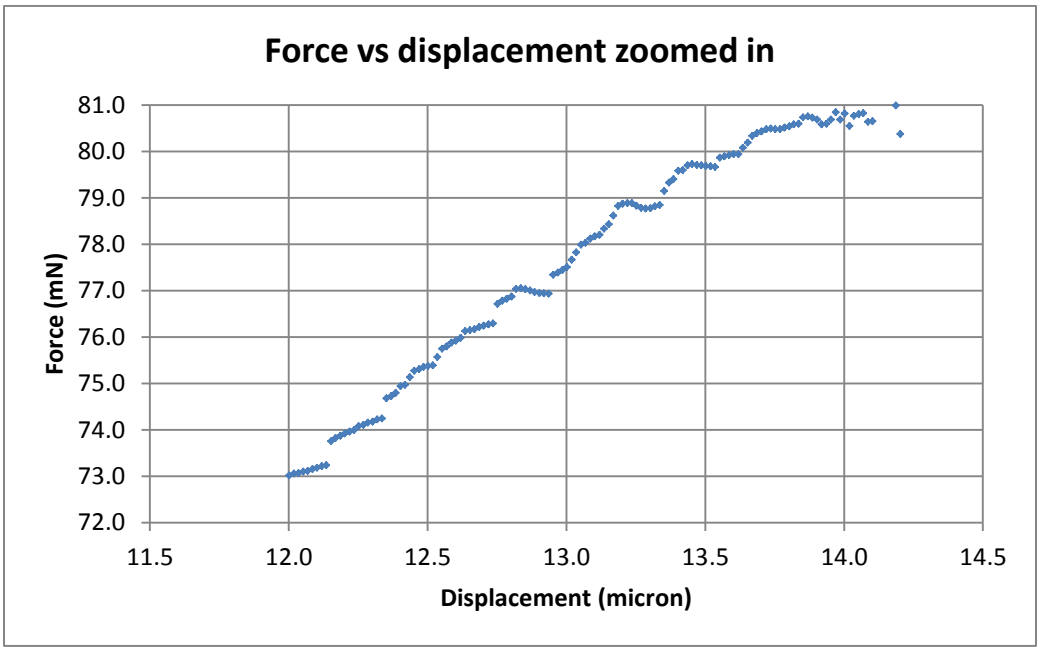

Figure 29: A closed up of a section of force-displacement curve

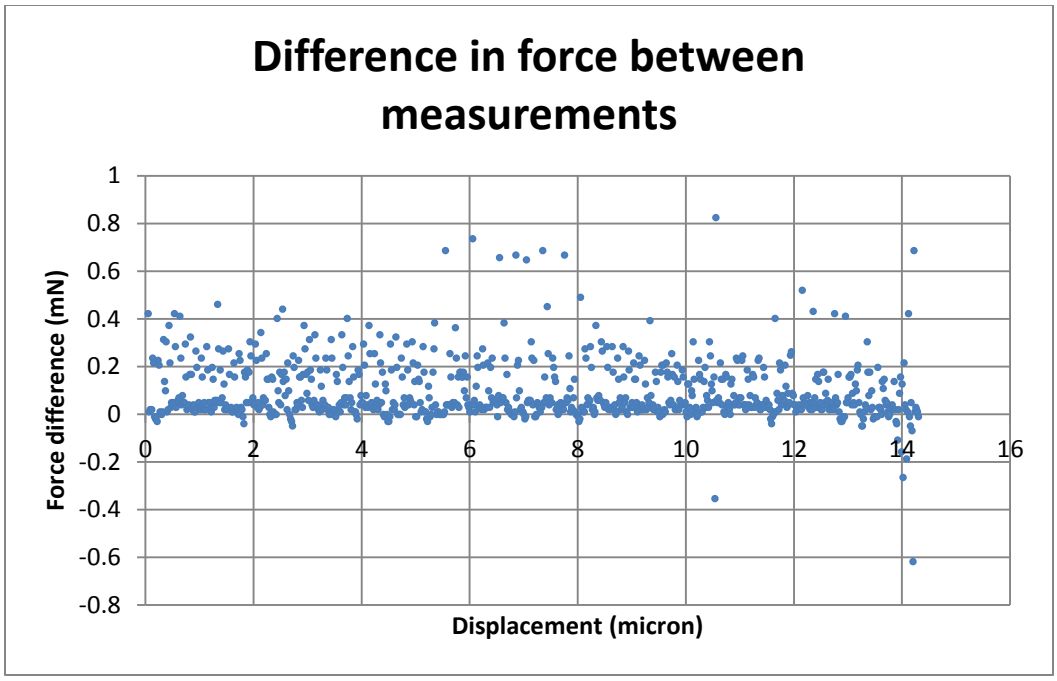

Figure 30: Difference in force magnitudes between measurements

Two MSA pulling experiments were conducted, one in 300 ppm Si ion concentration solution at pH 2.7, and the other in 200 ppm Si ion concentration solution. In the first test with 300 ppm solution, the cubes were aged for 3 weeks. The result was shown in **Figure 31**. The tensile force measured by MSA peaked at 55 microns of separation between cubes with a magnitude of 92.230 N. Immediately after the peak, the force returned to a relatively constant value of around 91.7 N till the end of the test. The maximum drop in force was measured at 0.53 N. SEM images of cubes at the end of the experiment showed growth of silica polymers on cube surfaces, shown in **Figure 32**.

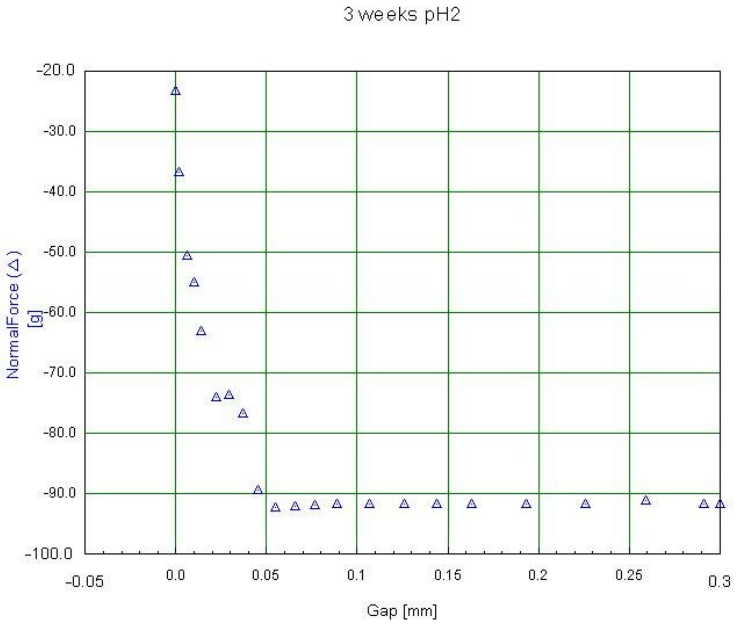

Figure 31: Force-displacement curve of MSA test 1

Figure 32: SEM image of cube surface after MSA test 1

In the second MSA pulling experiment, in 200 ppm solution, the cubes were aged for 4 weeks. The tensile force peaked at 91.690 g (equivalent to 0.899 N) when the cubes were separated by 22 microns. The maximum drop in force from the peak value to the

post-peak average value was 0.342 g (equivalent to 3.36 mN). The force-extension curve was shown in **Figure 33**.

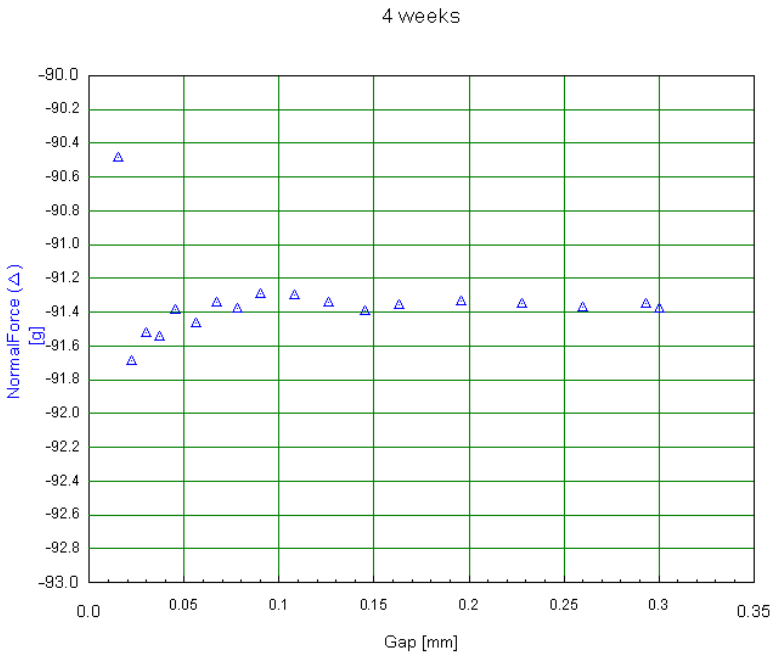

Figure 33: Force-displacement curve for MSA test 2

5.5. Mica-induced silica gel growth

Research by Israelachvili had shown that a difference in electrochemical potentials between compressed mica-silica surfaces induced dissolution of silica. Since clay particles are almost ever present in common soils, we decided to introduce muscovite mica as an experimental parameter into cube crushing experiments. A sheet of muscovite mica around 30 μm thick was inserted between silica cubes in pneumatic crusher prior to compression. The results are described below.

In 500 ppm Si ion concentration solution with pH value 5.0, two silica cubes were compressed with a mica sheet and aged for 3 weeks. **Figure 34** showed the results.

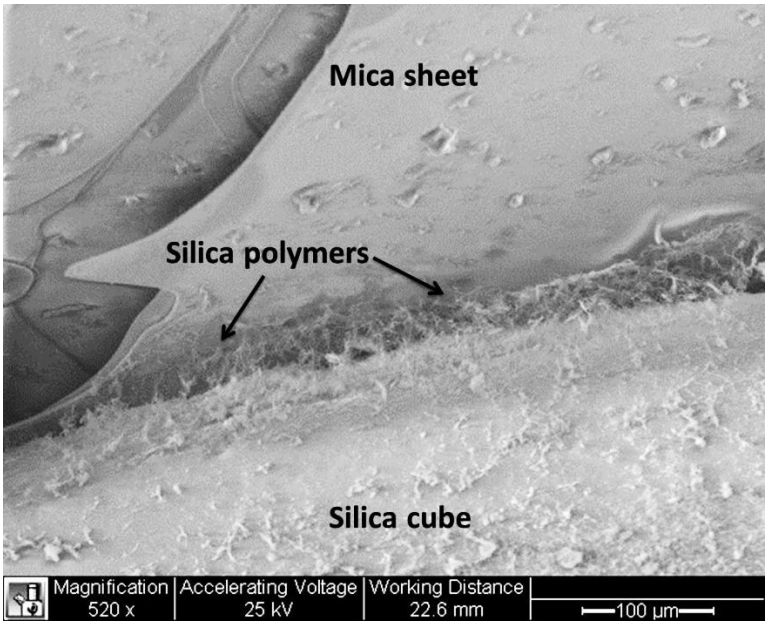

Figure 34: SEM image of cube-muscovite contact after aging

Clusters of thick silica fibers were seen growing between silica cube surface and mica sheet near the contact region. There was good contact between silica and mica, as the mica sheet was punctured and fractured at the contact point with both silica cubes. Further away from the contact region, the mica sheet appeared to be clean whereas the cubes were still covered by thin polymers. Interestingly, silica polymers 10s of μm in length were also seen growing near contacts between silica cube and stainless steel chamber. Furthermore, an extensive gel network was observed growing around one edge of a cube free from any compressive forces. The network had interconnected chambers with an overall dimension in the order of 100 μm.

In 300 ppm Si ion concentration solution with pH value 5.0, two silica cubes were compressed with a mica sheet and aged for 2 weeks. The results are shown in **Figure 35**.

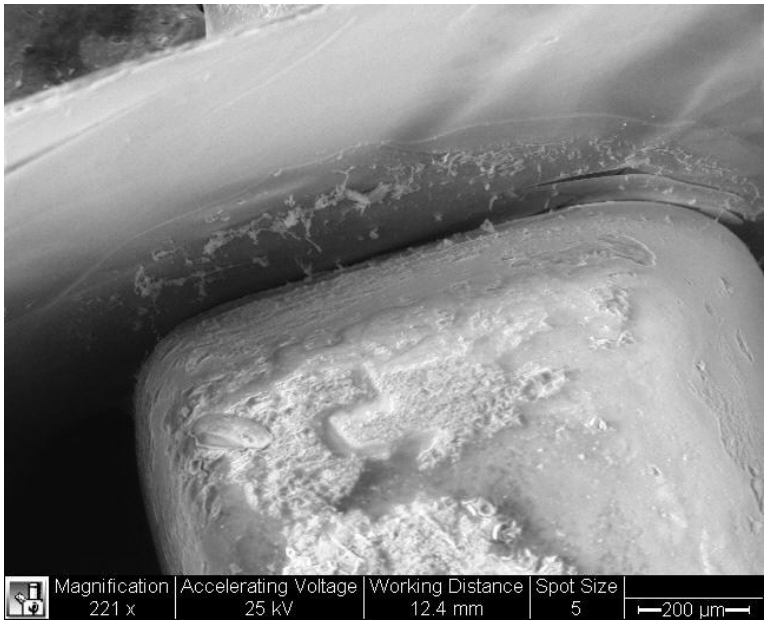

Figure 35: SEM image of mica sheet compressed between silica cubes

There was no big clusters of silica polymers growing anywhere in the liquid chamber. Instead, small polymers with lengths in the order of 10 μm were seen attached to both cube and mica surface. It was also clear that such growth of silica polymers was only near contact sites. Further away from the contact site between cube and mica sheet, no polymers were seen growing on mica sheet. There was another contact point between mica sheet and stainless steel chamber where mica sheet was punctured. No silica polymer growth was observed there.

The same test was repeated in solution with 200 ppm Si ion concentration and pH 5.0 for 3 weeks. As can be seen in **Figure 36**, silica polymers similar in size and were

observed growing on cube surfaces. But no polymer was found on mica sheet, and the density of polymers was lower than that in solution with 300 ppm Si ion concentration.

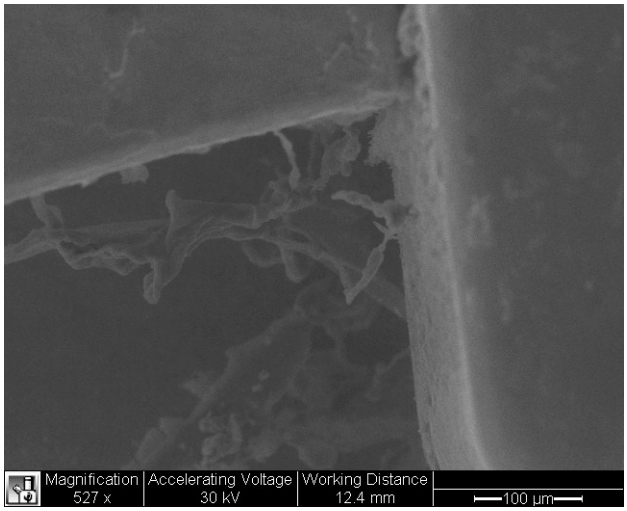

Figure 36: SEM image of cube surface after compression with mica sheet

In another test, the Si ion concentration in the solution was further reduced to 100 ppm. Two cubes were compressed with a mica sheet and aged for 4 weeks. No lengthy polymers were observed in the vicinity of contact region this time, but there were a few patches of small silica gel structures seen near the puncture site on mica sheet (**Figure 37**). The small patches of silica gel had dimensions in the order of 10 μm with some as small as 5 μm, and had many tiny interconnected chambers. An EDS analysis confirmed that the structures seen in the microscope was indeed silica, with minor traces of magnesium, potassium, aluminum, oxygen, nitrogen, and iron. Minor traces of carbon was also detected which proved that the structure was not biological and the carbon was likely from the environment when the liquid chamber was transported to SEM.

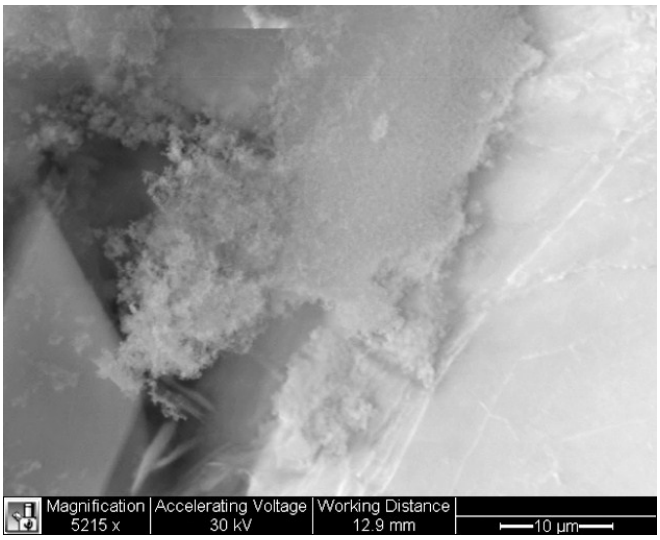

Figure 37: SEM image of silica polymers on mica sheet near stressed contact

Mica sheet was also inserted in a spring cube crushing experiment to test if the extra growth of silica gels, if any, created by the mica-silica contact would contribute to the adhesive force between the two cubes. Two spring cube crushing tests were conducted. In the first test, cubes were aged for 3 weeks in pH 2.7 300 ppm Si ion concentration solution and the results were shown in **Figure 38**. The force-extension curve had an upward slope until a maxima of 36.20 mN was reached, at which point the two cubes were separated by 0.6 mm. Zooming in to the force curve revealed an up-and-down force pattern (**Figure 39**). Differences in force magnitudes between adjacent points were taken and plotted in **Figure 40**. There was a trend where larger decreases occurred in the early stages of the pulling experiment. As the cubes became more separated, the magnitudes of decreases in mass became smaller and smaller. The largest increase in force was recorded at 0.481 mN at 141.7 μm extension.

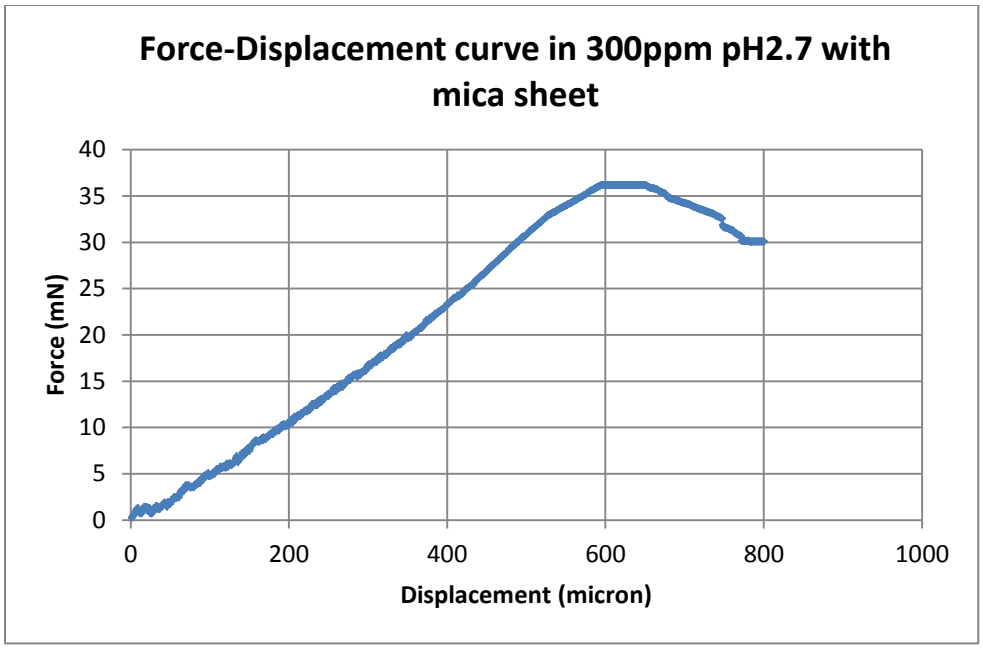

Figure 38: Force-displacement curve of cubes aged with mica sheet, Si 300 ppm

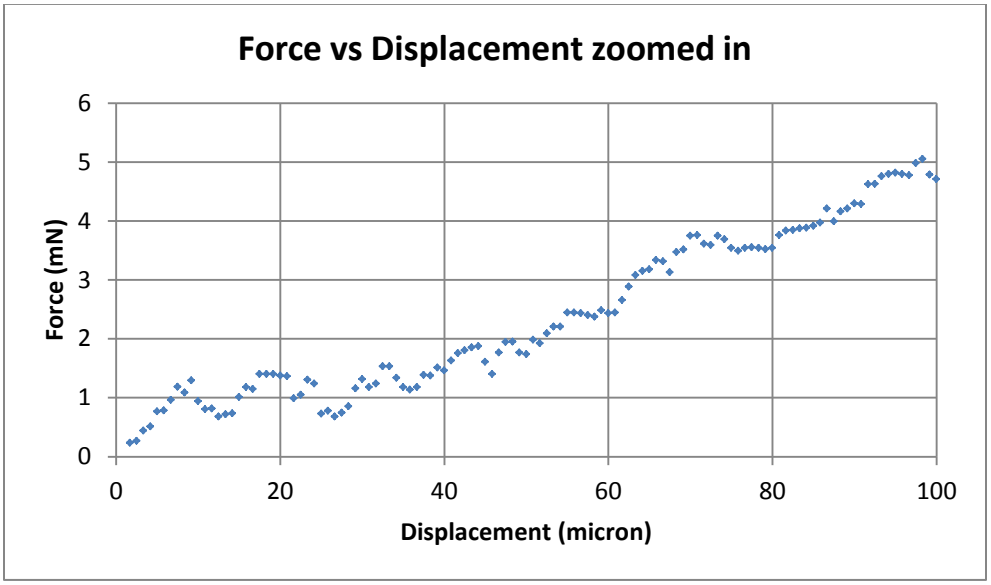

Figure 39: A section of force curve in Figure 38

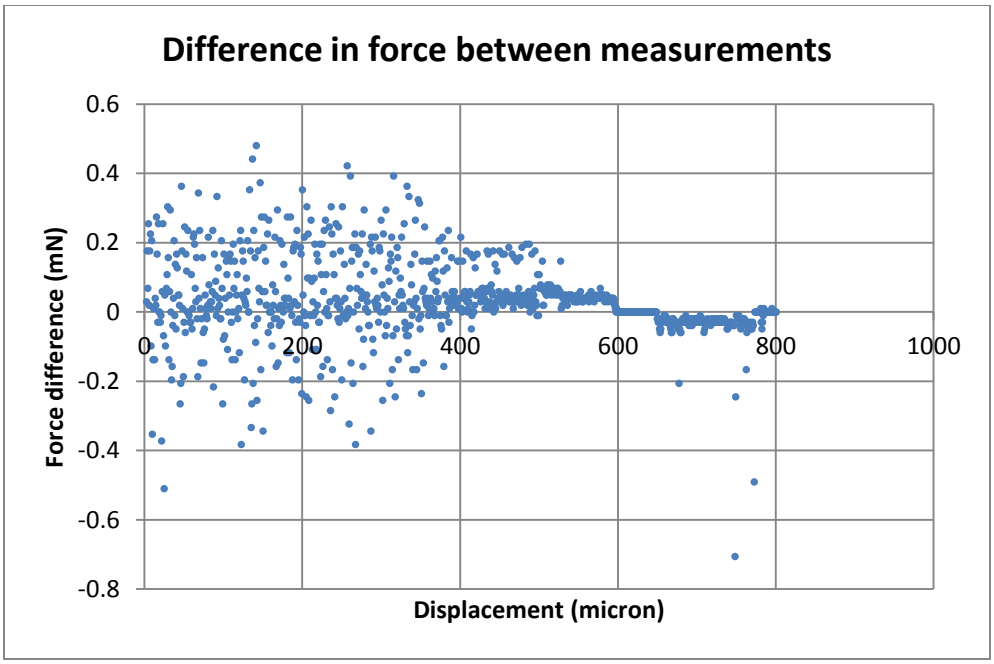

Figure 40: Difference in force magnitude in aging with mica measurements

In the second test, the pH value was 5.0. The result was shown in **Figure 41**. The force-extension curve showed two peaks of 26.7 mN at 0.063 mm extension, and 28.9 mN at 0.12 mm extensions. After the second peak, force started to drop in step-like patterns. There were four large drops in force magnitude which were 9.9 mN, 3.6 mN, 3.3 mN, and 3.3 mN respectively. In between these sudden drops, the force curve had small negative gradient. The cube displacements between these four large drops were 0.33 mm, 0.15 mm, 0.18 mm respectively. After the last drop in force magnitude, the force continued to decrease only slight as the two cubes were well separated from 0.86 mm onwards. SEM images of the cubes were taken after the test was completed and shown in **Figure 42**. It can be observed that large amount of silica gel structures had grown on mica sheet and around mica-silica contacts.

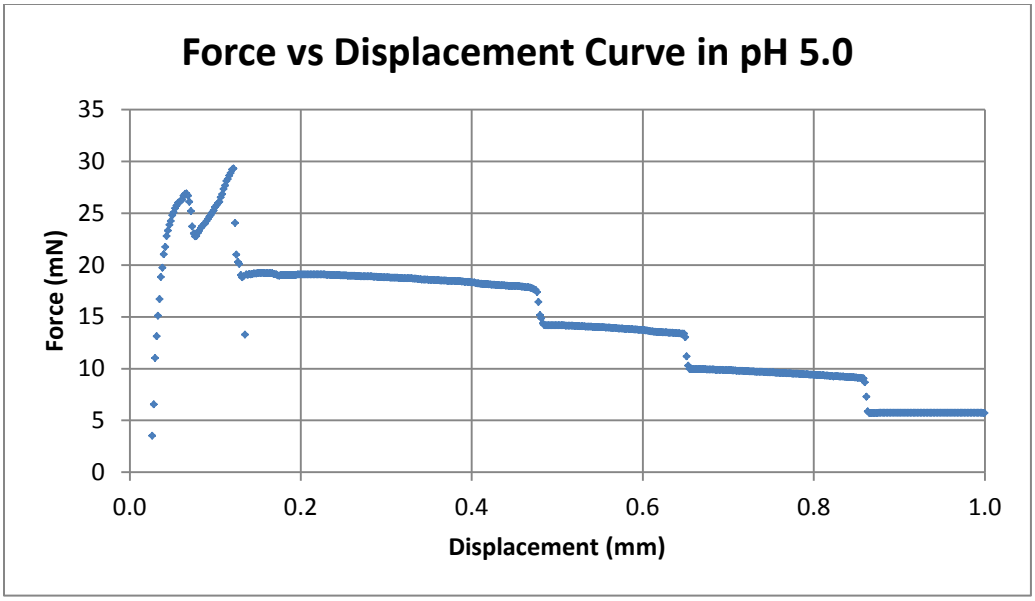

Figure 41: Force-displacement curve of cubes aged with mica, pH 5.0

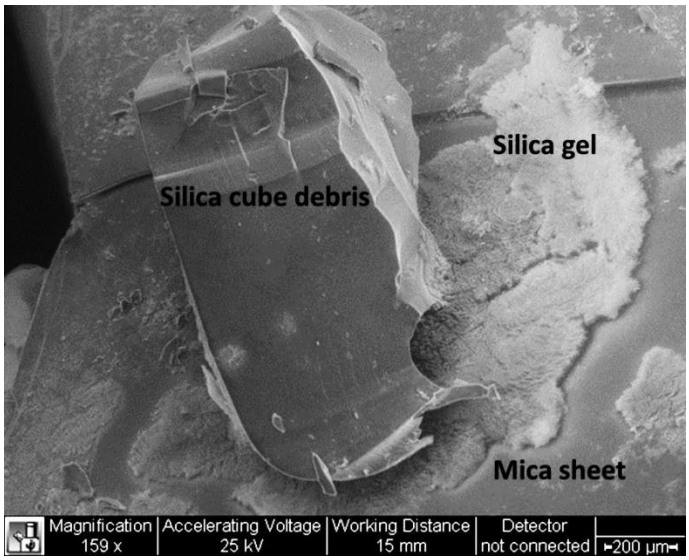

Figure 42: SEM image of silica-mica contact after 3 weeks aging in pH 5.0 Si 300 ppm solution

In 200 ppm Si ion concentration solution with pH 2.5, two cubes were compressed with a mica sheet for 3 weeks. SEM wet mode was used where the

microscope chamber was filled with low level of water vapor at low temperature to ensure samples did not dry out during imaging. **Figure 43** was captured in this mode. Small amount of silica polymers in hydrated forms were seen growing between silica cube and mica sheet. Some polymers were as long as 100 μm. small silica polymers had covered the surface of mica sheet near contact region.

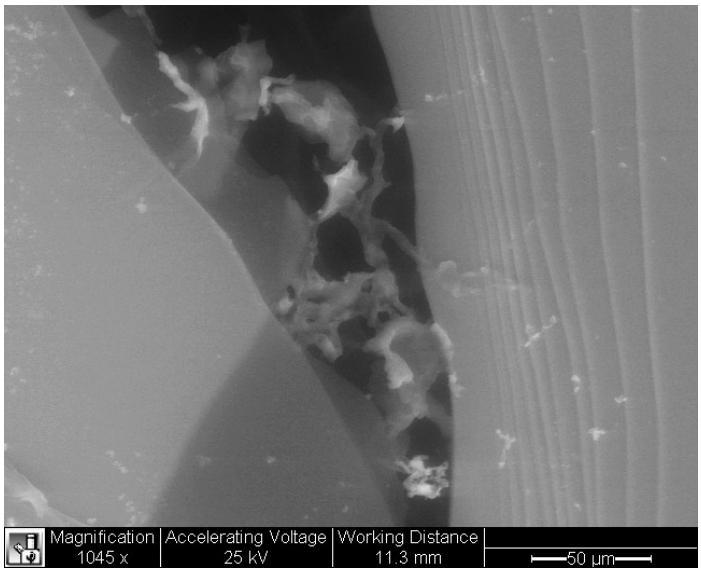

Figure 43: Hydrated silica polymers near contact in SEM wet mode

In another spring crushing test, instead of using mica sheet, 2 g of mica powder (No. 500 mesh, S&J Trading NY) was mixed with solution containing 200 ppm Si ion concentration at pH 2.5. After 3 weeks of aging, no obvious silica structures were seen in SEM imaging. Data for the force-extension curve is still been processed.

6. Discussion and conclusions

The silica gel growth in undisturbed solution experiments provided a qualitative bench mark for measuring the amount of silica gel in an experiment. In solution with 180 ppm Si ion concentration, it took seven days for small silica seeds to form. In 300 ppm or 500 ppm Si ion concentration solutions in pH 5.0, silica gel can be observed by the naked eye 2 weeks after experiments started. These observations served as an initial verification to our hypothesis that silica gel was able to grow in solution in the same amount of time that aging phenomenon was observed in soil found in literature. No silica gel was observed growing on silica cube surfaces in solutions with Si ion concentration below 150 ppm. Therefore in subsequent experiments conducted in solutions with Si ion concentration below 150 ppm, any observation of silica gel or polymers on silica surfaces can be attributed to accelerated silica dissolution or polymerization by the tests conducted. Observations made by AFM and SEM also provide an initial estimate that silica polymers were at least 10 nm thick.

In spring cube crushing experiments conducted in 500 ppm Si ion concentration solution, polymers a few hundred micrometers in length were found near the contact region. It can be seen in Figure 13 that silica polymers in the contact region adhered to both the left and right silica cube. Such a configuration would create adhesion between silica cubes at the microscopic level and thus enhance the granular strength of sand. In another experiment using the same set-up but in 300 ppm Si ion concentration solution,

deposits of silica gel were found in cube cracks (see Figure 16). Such deposits were roughly one magnitude smaller than those found in 500 ppm solution.

To determine how much effect stressed contact region had on precipitation and polymerization of silica, another cube crushing experiment was conducted in 300 ppm SI ion concentration solution. The compressive force applied to the cubes in this test was small enough to be able to bring the two cubes firmly together without damaging either cube. This way the level of stress at silica-silica contact region was kept to a minimum. No cracks were found on either cube after 2 weeks, and no silica gel deposits were seen anywhere on cube surfaces (see Figure 17). Therefore it was shown that the rate of silica precipitation and polymerization in the stressed contact region was higher when the stress between cubes was higher, most likely due to extra surfaces and asperities forming as a result of the stress.

Images taken from cube crushing experiments conducted in 200 ppm Si ion concentration at pH 2.5 showed extensive silica gels attached to cube surfaces as well as attached to very thin silica fibers (Figure 19). The results indicated that once grown, silica gels did exert an adhesive force to neighboring silica cubes. This was a further verification that silica gels grown in stressed contact regions can exert bonding forces to grains.

In AFM pulling experiments, step-like force patterns during cantilever withdrawal (see Figure 21) suggested that clusters of polymers were present on the surface. When the tip picked up a cluster of polymers, the polymers were stretched with

increasing force until one segment broke, at which point a sudden reduction in force was measured. As the tip was raised higher and higher from the stage, more polymers were stretched and broken, resulting in a step-like pattern. The maximum distances between withdrawing and approaching curves showed that the tensile strength of silica polymers was in the order of 100 nN. The distances between force peaks indicated that the length of those polymers was in the order of 100 nm.

Spring cube crushing experiments were designed to measure the intergranular adhesive force exerted by silica gels that grew in stressed silica cube contacts. In the experiment in solution with 500 ppm Si ion concentration, data near the peak in the force-extension curve (see Figure 24) can be used to estimate the size and strength of silica gels since that was when two cubes were almost separated with nothing but silica gels still attached to them. We believe that the force magnitudes of the five kinks near the peak of the curve, 66.7 μN, 22.6 μN, 27.5 μN, 180 μN, and 79.5 μN respectively, indicated the tensile strength of five clusters of silica gels. The horizontal distances between those kinks, 25.9 μm, 26.6 μm, 31.7 μm, and 36.5 μm respectively, indicated the length of those gel structures at full stretch.

We postulated that the initial force peak at 0.1172 mm was higher than subsequent force readings because up till that point silica structures between two cubes were undamaged and therefore yielded to a higher tensile force. It was also noticeable that after each kink, the distance to the next kink increased slightly. This may be because

shorter silica polymers were broken first, leaving longer polymers to be broken at larger separating distances.

The force curve from a second experiment conducted in the same conditions looked much different from that of the first (see Figure 26). The force difference curve showed that larger drops in force magnitudes occurred near the beginning of the pulling experiments (see Figure 27). The rationale behind plotting the differences in force magnitudes was that, when a silica polymer connecting to both cubes was broken, the analytic scale would record an increase in mass which was equivalent to a reduction in tensile force between cubes. Therefore the difference in force magnitudes was an indication to silica polymer strength. One way to explain this data was that more silica gels were damaged or broken when the cubes were first separated. As the separation process proceeded, fewer silica gel structures remained attached to both cubes, resulting in much smaller magnitude of decrease in force measured. The magnitude of decreases in mass can be converted to forces in the order of 100 μN. This force was another estimation of the strength of silica gel structures. Clearly the two explanations for the two different force-displacement curves contradicted each other. More experiments are needed to verify these theories.

Two more cube pulling experiment were conducted where the cubes were aged for three weeks in 300 ppm Si ion concentration solution. In the first experiment, the solution had a pH value of 2.5. The final separation distance between the two cubes was 14.3 μm (see Figure 28). Taking a closer look at the force curve (see Figure 29), it was

found that there still existed a step-like force pattern, similar to those seen in AFM pulling experiments. The average magnitude of sudden increase in forces was 0.5 mN. This was another estimation to the tensile strength of silica polymers growing between cubes.

Interpreting data from MSA tests remained a challenge. The machine only took measurements a certain amount of time which was preset. Due to the fact that silica polymers were extremely short, pulling tests had to be conducted at very slow speed, resulting in one measurement taken only every 5 to 15 seconds. Important data showing force patterns near separating point would be missed between measurements. We are currently in the process of perfecting the system to capture more force data during pulling. But the data still showed a peak in force right before the cubes were completely separated (see Figure 31, 33). Taking off surface tension recorded by a control experiment, MSA recorded a difference of 2.06 mN between the peak force and the first data point immediately after the peak, indicative of the granular strength of silica gel developed between two cubes.

Comparing SEM images of cubes after they were compressed and aged with and without mica sheets showed that, more silica polymers and gels were seen growing near mica-silica contacts. It was also observed that silica polymers were more likely to grow in the vicinity of stressed contacts on mica sheet (see Figure 34, 35, 37, and 42). Further away from the contact regions, no polymers were seen on mica sheet. Such phenomenon may be due to accelerated dissolution of silica in stressed contact regions and

subsequent precipitation near contact regions. It indicated the important role of the stressed contacts in the dissolution, precipitation, and polymerization of silica.

Two spring cube crushing experiments were conducted with a mica sheet between silica cubes. In the first one, the solution had a pH value of 2.7. The force curve had tiny kinks until the displacement between cubes reached 400 microns, after which the curve was smooth indicating no more polymers were still attached (see Figure 38). Zooming in on the section of force curve before 400 microns displacement, sudden small drops in force magnitudes were revealed. Difference in force magnitudes between consecutive measurements showed large positive differences before the 400 microns mark. The maximum increase in force magnitude was 0.481 mN, at 142 μm displacement. This measurement agreed with other force curves obtained in similar test conditions, indicating that silica gel grown in such conditions had a tensile strength in the order of 0.1 mN.

In the second spring cube crushing experiment with mica sheet, the pH value of the solution used was 5.0. A step-like force pattern was obtained (see Figure 41). The drops in magnitudes of force from one step to the next indicated the strength of the gel structure being stretched, which were 3.6 mN, 3.3 mN, and 3.3 mN respectively. The lengths of the steps indicated the length of that particular silica gel being stretched, which was 0.33 mm, 0.15 mm, and 0.18 mm respectively. Subsequent SEM imaging of the cubes supported the interpreted data as large amount of silica gel structures were seen covering the surfaces of the cubes (see Figure 42).

Mica powder in solution did not have any obvious effect on silica polymer growth in cube crushing experiments. We postulated that it was because suspended mica particles in solution did not provide enough contact surfaces comparing with compression between silica cubes and mica sheets to make an impact. But in consolidation tests, mixing mica powder with sand grains may provide useful results as the chance for a good contact between mica and sand particles may be much higher.

The results presented here are only preliminary. However, they are very important, because for the first time we have a chain of observations that confirms a long-existing hypothesis that a stressed contact with microcracks generates dissolved silica in the contact (asperity) vicinity, which eventually polymerizes, forming a structure between the grains. Such structure is sufficiently strong to represent a significant increase of tensile strength or, through a rotational deformational mode, compressive strength within a period of time that is of the order of weeks. One of the most important findings is that the failure pulling force of a single chain of the polymer is 330-450 nN. At the grain scale, the failure force of the intergranular bond was found to be between 0.1-3 mN. Multiple interwoven polymer chains are contained in a single intergranular polymer bond. Notably, such a force is as much as 15 times higher than the typical capillary force between two spherical grains (8mm in diameter) at contact failure, being of the order of 0.2-0.8 mN (Hueckel et al. 2013).

7. Future work

Research continues especially in the area of gelation of silica in the intergranular space. Further experiments using spring cube crusher are being conducted in solutions with different silica ion concentrations to measure the granular adhesive tensile force developed during aging and the effect of changing silica ion concentration in the surrounding solution. We are also in the process of eliminating different environmental factors that may have resulted in the two distinctively different types of force-displacement curves obtained from multiple spring cube crushing experiments.

Impact of mica on the polymerization of silica in the vicinity of stressed contact is being further evaluated. Cube crushing experiments using mica sheet as well as mica powder are ongoing. SEM imaging will give us a more complete picture of the extent of clay's effects on polymerization process.

AFM pulling experiments will be conducted on cubes after aging in both the spring crushing and the pneumatic crushing devices to further investigate the adhesive tensile strength of silica polymers developed during aging. Such data will be collaborated with both granular adhesive forces between two cubes obtained using the two cube crushing devices and SEM images of post-aging contact region to verify and to quantify the contribution such chemo-mechanical coupling process has toward aging process on a macroscopic level.

Consolidation tests using a mixture of Ottawa sand and muscovite mica powder are underway to study the effect of mica clay on the soil aging process. The data collected will be compared with literature to identify aging process and how much clay affects such process. Water used in consolidation tests will be sampled to test for any change in silica ion concentration.

A numerical model will be developed to predict the magnitude of intergranular adhesive force exerted by silica gel growth based on data such as surrounding solution silica concentration level, stress between grains, and pH value of pore fluid. The density of silica polymers near contact region will be estimated via SEM imaging or AFM scanning. Combine that with contact surface area and tensile strength of polymer or gel structures will give an estimate to the intergranular adhesive force provided by the gel structures to grains. The model will also include the aging time and presence of mica. Simulated results will be compared with new experiment data as well as literature.

Bibliography

Baxter, C. D. P. and J. K. Mitchell (2004). "Experimental study on the aging of sands." Journal of Geotechnical and Geoenvironmental Engineering **130**(10): 1051-1062.

Becker, A. (1995). "Quartz pressure solution: influence of crystallographic orientation." Journal of Structural Geology **17**(10): 1395 - 1405.

Bjorkum, P. (1996). "How important is pressure in causing dissolution of quartz in sandstones?" JOURNAL OF SEDIMENTARY RESEARCH **66**({1, Part a}): 147-154.

Bowman, E. T. and K. Soga (2003). "Creep, ageing and microstructural change in dense granular materials." Soils and Foundations **43**(4): 107-117.

Denisov, N. Y. and B. F. Reltov (1961). "The influence of certain processes on the strength of soils." Proceedings of the 5th International Conference of Soil Mechanics and Foundation Engineering **1**: 75-78.

Gratier, J., et al. (2009). "A pressure solution creep law for quartz from indentation experiments." J. Geophys. Res. **114**(B3): B03403-.

Greene, G. W., et al. (2009). "Role of electrochemical reactions in pressure solution." Geochimica et Cosmochimica Acta **73**(10): 2862-2874.

Houseknecht, D. W., et al. (1987). "Relationships among Vitrinite Reflectance, Illite Crystallinity, and Organic Geochemistry in Carboniferous Strata, Ouachita Mountains, Oklahoma and Arkansas - Reply." Aapg Bulletin-American Association of Petroleum Geologists **71**(3): 347-347.

Hu, L. B. and T. Hueckel (2007a). "Coupled chemo-mechanics of intergranular contact: Toward a three-scale model." Computers and Geotechnics **34**(4): 306-327.

Hu, L. B. and T. Hueckel (2007b). "Creep of saturated materials as a chemically enhanced rate-dependent damage process." International Journal for Numerical and Analytical Methods in Geomechanics **31**(14): 1537-1565.

Hueckel, T., et al. (2005). Field derived compressibility of deep sediments of the Northern Adriatic. 7th International Symposium on Land Subsidence, Shanghai.

Hueckel, T., et al. (2001). "Aging of oil/gas-bearing sediments, their compressibility, and subsidence." Journal of Geotechnical and Geoenvironmental Engineering **127**(11): 926-938.

Hueckel, T., et al. (2013). Micro-scale study of rupture in desiccating granular media. Geo-Congress; Stability and Performance of Slopes and Embankments, San Diego, CA.

Iler, R. K. (1955). "The Colloid Chemistry of Silica and Silicates." Soil Science **80**(1): 86.

Krauskopf, K. B. (1956). "Dissolution and precipitation of silica at low temperatures." Geochimica et Cosmochimica Acta **10**(1-2): 1 - 26.

Kristiansen, K., et al. (2011). "Pressure solution - The importance of the electrochemical surface potentials." Geochimica et Cosmochimica Acta **75**(22): 6882-6892.

Mesri, G., et al. (1990). "Postdensification penetration resistance of clean sands." Journal of Geotechnical Engineering **116**(7): 1095-1115.

Meyer, E. E., et al. (2006). "Experimental investigation of the dissolution of quartz by a muscovite mica surface: Implications for pressure solution." JOURNAL OF GEOPHYSICAL RESEARCH-SOLID EARTH **111**(B8).

Mitchell, J. K. (1993). Fundamentals of soil behavior, Wiley.

Mitchell, J. K. and Z. V. Solymar (1984). "Time-dependent strength gain in freshly deposited or densified sand." Journal of Geotechnical Engineering-ASCE **110**({11}): 1559-1576.

Oelkers, E. H., et al. (1992). The Mechanism of Porosity Reduction, Styolite Development and Quartz Cementation in North-Sea Sandstones. 7th International Symposium on Water-rock Interaction, Park City, UT.

Parry, R. H. G. (2004). Mohr circles, stress paths and geotechnics. London, Spon Press.

Rubin, C. J. (2009). A Novel Apparatus for the Study of Intergranular Silica Microstructures. Durham, NC, Duke University.

Schmertmann, J. H. (1991). "The Mechanical aging of soils." Journal of Geotechnical Engineering **117**(9): 1288-1330.

Schott, J., et al. (2009). The Link Between Mineral Dissolution/Precipitation Kinetics and Solution Chemistry. Thermodynamics and Kinetics of Water-Rock Interaction. E. H. Oelkers and J. Schott. **70:** 207-258.

Soulie, F., et al. (2007). Effect of capillary and cement-led bonds on the strength of unsaturated sands. Experimental Unsaturated Soil Mechanics. T. Schanz. **112:** 185-193.

Wang, Y. H. and K. Y. Tsui (2009). "Experimental Characterization of Dynamic Property Changes in Aged Sands." Journal of Geotechnical and Geoenvironmental Engineering **135**(2): 259-270.

Wang, Y. H., et al. (2008). "Discrete element modeling of contact creep and aging in sand." Journal of Geotechnical and Geoenvironmental Engineering **134**(9): 1407-1411.

Worden, R. H. and S. Morad (2000). Quartz cementation in oil field sandstones: a review of the key controversies. Quartz cementation in sandstones. R. H. Worden and S. Morad. Malden, MA, Blackwell Science**:** 1-20.